



Deciphering the Mechanism of Action *Cosmos caudatus* Compounds Against Breast Neoplasm: A Combination of Pharmacological Networking and Molecular Docking Approach with Bibliometric Analysis

Wahyu Hendrarti¹, Abdul Halim Umar^{1,*}, Reny Syahrani¹, Mohamad Rafi², Wisnu Ananta Kusuma²

¹Almarisah Madani University, Makassar, South Sulawesi, Indonesia

²IPB University, Bogor, Indonesia

*Correspondence: E-mail: ahuhelim76@yahoo.com

ABSTRACT

Cosmos caudatus is a widely used traditional medicinal plant in Indonesia for cancer treatment. However, the mechanism of action of plants in treating breast neoplasms remains unclear. Thus, the active ingredients of *C. caudatus* and possible molecular pathways against breast neoplasms were investigated using pharmacological networks. The active compounds were screened using Lipinski and ADME parameters. Targets for the compounds were obtained using SwissTargetPrediction. Target diseases were identified using the Therapeutic Target Database, whereas disease pathways were analyzed using the Kyoto Encyclopedia of Genes and Genomes. Network pharmacology was constructed using Cytoscape. Protein-protein interactions were constructed using STRING. Gene ontology and KEGG were analyzed using DAVID. Molecular docking confirmed that the compounds and targets exhibited the best interactions. The compounds, targets, and pathways with the highest degrees in the breast neoplasm network were eriodictyol, ABCC1, and signal transduction, respectively. EGFR is the key target of PPIs. GO enrichment in BP, MF, CC, and KEGG regulated NF-KB transcription factor activity, chromatin, transcription coactivator binding, and pathways in cancer, respectively. Molecular docking with the best score on interaction 5-O-methylvisammioside-SLC2A1 (PDB ID: 6THA) (-10.3 kcal mol⁻¹). The compound 5-O-methylvisammioside may have pharmacological activity in breast cancer through signal transduction pathways.

ARTICLE INFO

Article History:

Submitted/Received 02 Apr 2024

First Revised 20 May 2024

Accepted 01 Jul 2024

First Available online 02 Jul 2024

Publication Date 01 Sep 2024

Keyword:

Bioinformatics,

Breast cancer,

Breast neoplasm,

Drug-likeness,

Pharmacological mechanism,

Signaling pathway.

1. INTRODUCTION

Cosmos caudatus (Asteraceae) is known as a kenikir in Indonesia. It has been widely used in traditional medicine because of its pharmacological activities and beneficial effects on human health. This plant, mainly its leaves, is widely utilized for treating diabetes, osteoporosis, hyperlipidemia, cancer, and hypertension; and is used as an antibacterial, antifungal, antioxidant, and anti-inflammatory agent. The leaves can be consumed in the form of fresh vegetables or tea drinks, either alone or in combination with other plants (Ahda et al., 2023; Cheng et al., 2015; Firdaus et al., 2021; Rafi et al., 2023; Sharifuldin et al., 2016; Yusoff et al., 2021), as well as anti-aging skin (Loo et al., 2023). The potential of this plant is even more promising because of its shallow toxic effects and because it can be consumed without risk (Ahda et al., 2023; Cheng et al., 2015; Herlina et al., 2021). Many in vitro tests, in vivo experiments, and clinical trials have been conducted to confirm the potential of this plant (Ahda et al., 2023).

The leaves of this plant have been reported to contain compounds such as flavonoids and their derivatives, other phenolics, and volatile oils (Ahda et al., 2023; Firdaus et al., 2021; Rafi et al., 2023; Seyedreihani et al., 2017; Sharifuldin et al., 2016). Metabolomic approaches identified compounds such as quercetin, kaempferol, myricetin, catechin, luteolin, apigenin, quercetin 3-O-rhamnoside (quercitrin), quercetin 3-O-glucoside, quercetin 3-O-arabinofuranoside, rutin, phenolic acid, chlorogenic acid, α -Linolenic acid, myo-inositol, diterpenoids, costunolide, and stigmasterol which have potential in the treatment of diabetes mellitus (Ahda et al., 2023; Cheng et al., 2015). Essential oils such as α -Cadinene, (E)-Ocimene, 2,6-Dimethyl-1,3,5,7-octatetraene, α -Copaene, β -Elemene, caryophyllene, α -Humulene, γ -Muurolene, Bergamotene, β -Selinene, Bicyclogermacrene, α -Farnesene, δ -Cadinene, stigmasterol, lutein, 4,4' bipyridine, and costunolide which have reported to possess antimutagenic, antimicrobial, and antifungal properties (Ahda et al., 2023; Lee & Vairappan, 2011; Yusoff et al., 2021). Quercetin glycosides, chlorogenic, neo-chlorogenic, and cryptochlorogenic compounds act as antioxidants (Firdaus et al., 2021; Rafi et al., 2023; Shui et al., 2005; Widiyantoro & Harlia, 2021). Catechin, quercetin, rutin, kaempferol, and chlorogenic acid are antihyperlipidemic compounds (Rahman et al., 2017). Ascorbic acid, quercetin, and chlorogenic acid are anti-inflammatory (Cheng et al., 2015). *C. caudatus* leaf extract is reported to have activity against HeLa cells, so it has enormous potential for inhibiting cancer cell proliferation, especially breast cancer. Nevertheless, the molecular profile of the compound, target, disease, pathway, and their mechanisms remain unknown. Networking pharmacology and molecular docking methods can offer a preliminary understanding of the underlying mechanisms.

Pharmacological networking is a comprehensive approach that can predict the interactions between compounds, target genes, diseases, and pathways, thus providing an overview of the mechanisms underlying the treatment of a particular disease. On the other hand, molecular docking is a computational technique to predict the best interaction and binding affinity between a ligand and a protein. The combination of both can provide scientific support and new technologies for rational clinical drug use and development (Huang et al., 2024; Syahrani et al., 2023; Umar et al., 2023). In this study, we explored the possible active compounds, targets, diseases, and pathways, as well as the molecular mechanisms of the active compounds in treating breast neoplasms using pharmacological networking and molecular docking. The research experiments' flowchart is shown in **Figure 1**.

To support this research, a bibliometric analysis was performed to understand the trend and development of research on integration network pharmacology and molecular docking

in breast neoplasm treatment. Bibliometric analysis has been widely applied to support various types of research (Demir *et al.*, 2024; Ellili, 2024; Husain *et al.*, 2023; Lim & Kumar, 2024; Sahidin *et al.*, 2023; Solihah *et al.*, 2024).

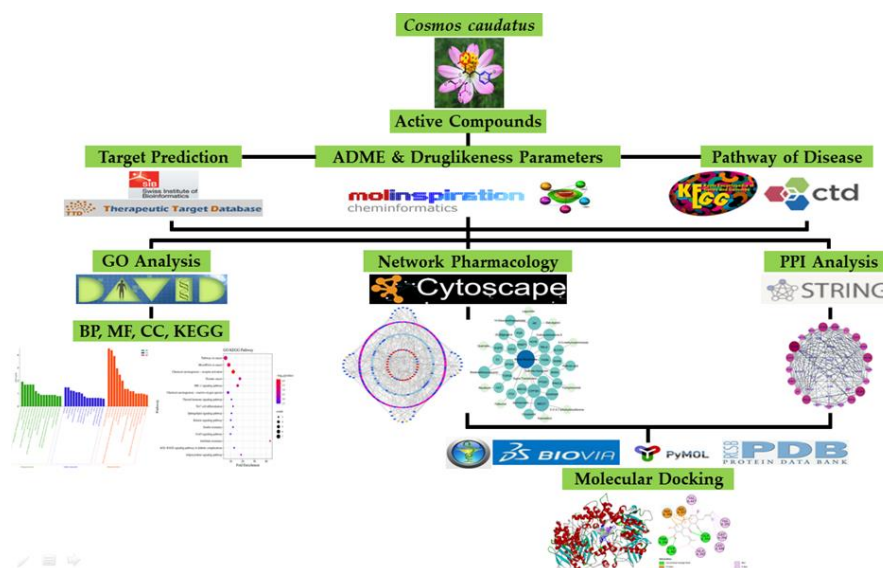


Figure 1. Flowchart of the current research exploring the mechanisms of action of compounds from *Cosmos caudatus* for the treatment of breast neoplasm by network pharmacology and molecular docking. GO (gene ontology), BP (biological process), MF (molecular function), CC (cellular component), KEGG (Kyoto encyclopedia of genes and genomes), PPI (protein-protein interaction), ADME (absorption, distribution, metabolism, and excretion).

2. METHODS

2.1. Bibliometric literature review analysis

Bibliometric analysis was used to support this research. The method used refers to Al Husaeni & Nandiyanto (2022). This analysis uses Publish or Perish (PoP) ver. 8.12.4612 (<https://harzing.com/resources/publish-or-perish>) and VOSviewer ver. 1.6.20. (<https://www.vosviewer.com/>), a Google Scholar database with the keywords “network pharmacology and molecular docking” from 2017–2024 (last seven years), and a maximum of 1000 results (including citations and patents). The data was downloaded and converted into *.csv and *.ris formats. Fields from which terms will be extracted by title and abstract fields, counting method using binary counting, the minimum number of occurrences of a term by five (threshold).

2.2. Chemical compounds of *Cosmos caudatus*

Through a metabolite profiling approach, we collected the chemicals we discovered from *Cosmos caudatus* from our earlier study (Rafi *et al.*, 2023). Online databases, such as ChemSpider (<http://www.chemspider.com/>) (Pence & Williams, 2010), PubChem (<https://pubchem.ncbi.nlm.nih.gov/>) (Kim *et al.*, 2016), KNApSACK Family (http://www.knapsackfamily.com/KNAPsACK_Family/) (Afendi *et al.*, 2012), Molbase (www.molbase.com), SpectraBase (<https://spectrabase.com/>), and Traditional Chinese Medicine Systems Pharmacology Database and Analysis Platform (TCMSP) (<https://tcm-sp-e.com/tcm-sp.php>) (Ru *et al.*, 2014) provided the chemical structures and compound IDs. If

these formats were not discovered in the database, chemical structures were further examined using MarvinSketch 19.6 (<https://chemaxon.com/products/marvin>) to retrieve canonical SMILES and PDB subsequently, using the acquired data in the form of compounds, canonical SMILES, and compound IDs. In this case, a database is created (Umar et al., 2023).

2.3. Drug-likeness prediction of absorption parameters of the chemical components of *Cosmos caudatus*

Molinspiration Cheminformatics was used to calculate the absorbance parameters (physicochemical properties, lipophilicity, and drug-likeness) to follow the "five principles" of drug absorption: relative molecular mass (BM) ≤ 500 , hydrogen bond acceptors (nON) ≤ 10 , hydrogen donors (nOHNH) ≤ 5 , molar refractivity 40-130, coefficient partition in water-lipid (miLogP) ≤ 5 , and bioavailability $\geq 30\%$ (Syahrini et al., 2023). Only compounds that met the absorption parameters were analyzed in this study.

2.4. Screening and prediction targets

The Swiss online platform databases Target Prediction (<http://swisstargetprediction.ch/>) (Daina et al., 2019) and SuperPred (<http://prediction.charite.de/>) (Nickel et al., 2014) were used to target candidate compounds that satisfied absorbance requirements (in the form of canonical SMILES). For network analysis, the top ten targets from the screening of the findings were selected.

2.5. Disease activity screening

The selected targets were subsequently evaluated using the Therapeutic Target Database (TTD) (<https://db.idrblab.org/ttd/>) (Chen et al., 2002) and the Comparative Toxicogenomics Database (CTD) (<http://ctdbase.org/>) (Davis et al., 2023) to acquire the disease categories of targets that fulfill the requirements. Next, a network was constructed using the top ten target disease candidates identified at this stage.

2.6. Screening and prediction of disease pathways

The Kyoto Encyclopedia of Genes and Genomes (KEGG) (<https://www.genome.jp/kegg/>) (Kanehisa & Goto, 2000) was used to examine data from the top ten diseases produced by TTD and CTD analysis (p -value < 0.01) for disease pathways. Disease pathways linked to breast neoplasms were predicted using the top ten disease pathways.

2.7. Compound–target–disease–pathway network construction

To construct multi-compound–multi-target, multi-target–multi-disease, and multi-disease–multi-pathway interaction networks, the active compounds of *C. caudatus* were imported into Cytoscape 3.10.1 software together with their possible targets, diseases, and pathways. The network was analyzed using Network Analyzer (Umar et al., 2023) and visualized using Cytoscape ver. 3.10.1 (<https://cytoscape.org/>). The network connections generated were assessed using topological properties such as degree, betweenness centrality, and closeness centrality values (Chen et al., 2024).

2.8. Construction of a protein-protein interaction network

The gene/protein interactions of the primary targets derived from *C. caudatus* were identified using the STRING search tool version 11.0 (<https://string-db.org>). With the highest degree of confidence, overlap was predicted, requiring a minimum interaction score of 0.900 (*Homo sapiens*). The protein-protein interaction (PPI) networks might be visualized by

exporting the PPI data from STRING with a threshold of >0.4 to Cytoscape ver. 3.10.1 (Shannon *et al.*, 2003) by transferring the network to the Cytoscape tool. The significance of core targets is indicated by degree values in PPI network analysis. Umar *et al.* (2023) state that PPI networks use edges to describe protein-protein connections. The higher the number of lines in the network, the stronger the connection.

2.9. Gene ontology and pathway analysis

The Kyoto Encyclopedia of Genes and Genomes (KEGG) and Gene Ontology (GO) pathway analyses were carried out using STRING ver. 11.0 (<https://string-db.org>) (Szklarczyk *et al.*, 2019) and the DAVID Bioinformatics Resources 6.8 server (<https://david.ncifcrf.gov/home.jsp>) (Sherman *et al.*, 2022). GO enrichment was used to profile the biological process (BP), cellular component (CC), and molecular function (MF) terms of the retrieved targets. In contrast, KEGG pathway enrichment was utilized to identify significant biological pathways. The selected items have p-values and false discovery rate (FDR) values less than 0.01 (Umar *et al.*, 2023). The FDR was computed using the Bonferroni procedure. We selected the top 15 KEGG pathways or GO enrichments. The data was analyzed using SRplot (<http://www.bioinformatics.com.cn/en>) to illustrate the GO and KEGG enrichment results.

2.10. Molecular docking experiment

Compound CIDs and two-dimensional (2D) structures of ligands were taken from the PubChem data repository (<https://pubchem.ncbi.nlm.nih.gov/>) (Kim *et al.*, 2021) and the RCSB PDB (<http://www.rcsb.org/>) provided the proteins (receptors) that matched the targets (specific to Homo sapiens) (Goodsell *et al.*, 2020). These target genes' PDB IDs were obtained from the NCBI (<https://www.ncbi.nlm.nih.gov/gene/>) and the Protein Data Bank (PDB) (Burley *et al.*, 2017). Using the MMFF94 force field and Steepest Descent algorithm, ligand optimization was carried out using the Chimera-1.17.3 program (UCSF Chimera; <https://www.cgl.ucsf.edu/chimera/>). PyMOL version 2.5 (<https://pymol.org/2>) was utilized to make structural corrections to the protein, including eliminating ligands and water. PyRx AutoDock Vina (<https://pyrx.sourceforge.io/>) version was used to calculate the binding energy, RMSD, amino acid residues, and bond type for the optimized ligand and receptor. Furthermore, PyMOL and BIOVIA Discovery Studio Visualizer (<https://www.3dsbiovia.com>) were used to visualize the ligand and receptor docking results (Umar *et al.*, 2023). The lowest bond energy value (high docking value) and hydrogen bonds were selected as the best candidates.

3. RESULTS AND DISCUSSION

3.1. Bibliometric analysis

In the initial search, the selected threshold found 1798 terms, and 94 met the threshold. In 2024, publications on network pharmacology and molecular docking reached 77 articles (accessed on 25 May 2024). In 2023, the number of publications was 170. In 2022, the number of publications was 103.

The increase in research on network pharmacology and molecular docking can be used as a consideration for research, especially for traditional medicinal materials that will be carried out in the future. Considerations that can be made include whether the research trend regarding the pharmacological activity of natural materials is still relevant or not (Al Husaeni & Nandiyanto, 2022; Sahidin *et al.*, 2023).

A minimum of five was used for each term relationship in VOSviewer. The results of the VOSviewer analysis resulted in 51 items, 7 clusters, 575 links, and 3019 total link strengths. Cluster 1 resulted in 13 items, cluster 2 with 12 items, cluster 3 with 8 items, cluster 4 with 6 items, cluster 5 with 5 items, cluster 6 with 4 items, and cluster 7 with 3 items. Each cluster describes the relationship between two or more terms. VOSviewer has three different representations for bibliometric mapping. These representations include network, overlay, and density visualizations. The colored circles are labels for each keyword. The number of keywords in the title and abstract is closely related to the size of the circle. The size of each circle is closely related to the frequency of the keyword (Husain et al., 2023).

Figures 2a and 2b show the overlay and density visualization, respectively. In the overlay, the more recent the study, the brighter the visualized color. From the research data, the color of research below 2023 (2022.0–2022.6) is dark blue, while research entering 2023 is bright yellow. Figure 2a illustrates that research related to network pharmacology has decreased, but the integration of network pharmacology with other fields such as molecular docking and cancer is still lacking. The density visualization (Figure 2b) shows that the research has a density visualization with high brightness (the denser), indicating that the keyword is used most often, and vice versa, if the color fades and blends with the background, the less often it is used in research (Al Husaeni & Nandiyanto, 2022; Muñoz-Leiva et al., 2012).

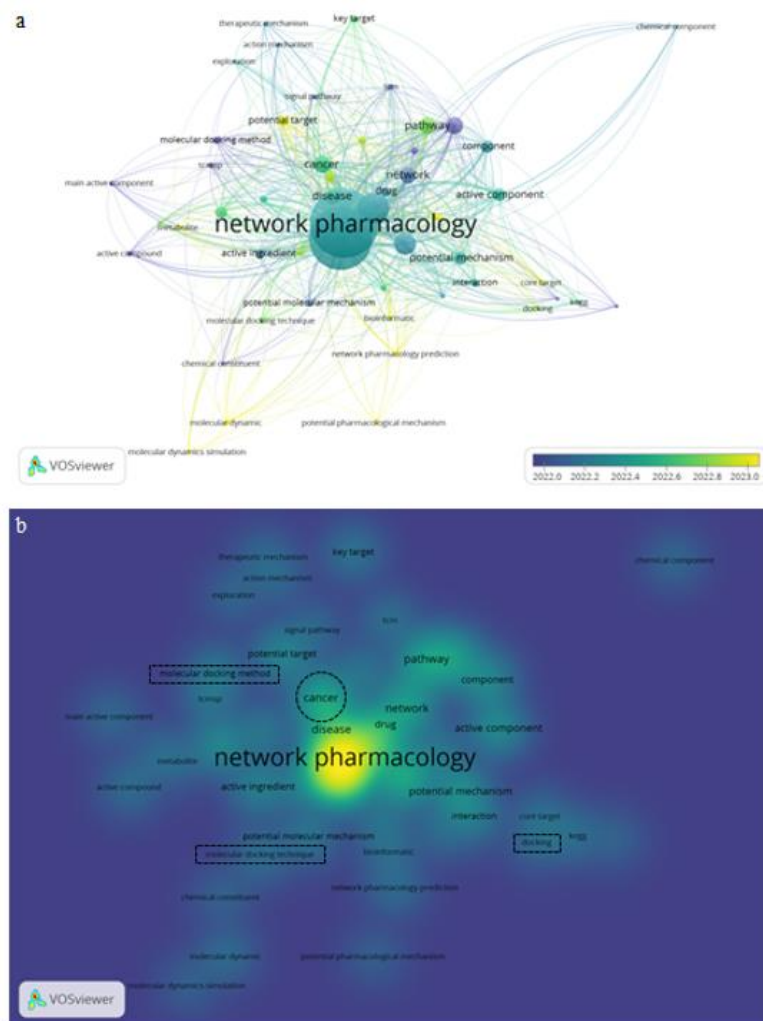


Figure 2. The visualization of the progress of network pharmacology and docking molecular research. (a) co-word map overlay visualization and (b) co-word map density visualization. The lighter the yellow color in (a) and (b), the more research is related to the item.

3.2. Active compounds of *Cosmos caudatus*

Using LC-HRMS for metabolite profiling, a total of 70 active compounds were extracted. Some alkaloid and steroid groups were among the detected chemicals, but phenolic and terpenoid groups predominated (Table 1).

Table 1. The absorption parameters of *C. caudatus* compounds use the Lipinski rule of five and the drug-likeness parameter.

No	Compound	Physicochemical Properties					Lipophilicity	Drug-likeness
		Molecular Formula	MW (≤500)	nON (≤10)	nOHNH (≤5)	MR (40–130)	Log $P_{o/w}$ (≤5)	Bioavailability ≥ 30%
1	Humulene (alpha)	C ₁₅ H ₂₄	204.35	0	0	70.42	4.53	0.55
2	Homononactinic acid	C ₁₁ H ₂₀ O ₄	216.27	4	2	56.90	0.75	0.85
3	Murolladien-3-One	C ₁₅ H ₂₂ O	218.33	1	0	69.24	3.46	0.55
4	Curcumenol	C ₁₅ H ₂₂ O ₂	234.33	2	1	69.25	3.04	0.55
5	Attractylenolide III	C ₁₅ H ₂₀ O ₃	248.32	3	1	69.15	2.47	0.55
6	Aloe-emodin	C ₁₅ H ₁₀ O ₅	270.24	5	3	69.92	0.10	0.55
7	Galaxolidone	C ₁₈ H ₂₄ O ₂	272.40	2	0	81.81	4.26	0.55
8	Norambreinolide	C ₁₆ H ₂₆ O ₂	250.38	2	0	73.49	3.80	0.55
9	Piperine	C ₁₇ H ₁₉ NO ₃	285.34	3	0	85.47	2.39	0.55
10	Luteolin	C ₁₅ H ₁₀ O ₆	286.24	6	4	76.01	-0.03	0.55
11	Kaempferol	C ₁₅ H ₁₀ O ₆	286.24	6	4	76.01	-0.03	0.55
12	2'-Methoxyformonetin	C ₁₇ H ₁₄ O ₅	298.29	5	1	82.93	1.01	0.55
13	Fallacinol	C ₁₆ H ₁₂ O ₆	300.26	6	3	76.41	-0.20	0.55
14	Retinoic acid	C ₂₀ H ₂₈ O ₂	300.40	2	1	95.28	0.00	0.00
15	Bisdemethoxycurcumin	C ₁₉ H ₁₆ O ₄	308.30	4	2	89.82	2.13	0.55
16	Triptophenolide	C ₁₅ H ₂₄ N ₂ O ₅	312.40	3	1	90.59	3.75	0.55
17	Isorhamnetin	C ₁₆ H ₁₂ O ₇	316.26	7	4	82.50	-0.31	0.55
18	(S)-[6]gingerol	C ₁₇ H ₂₆ O ₄	399.40	9	5	98.45	-4.37	0.55
19	Ceratodictyol	C ₁₉ H ₃₈ O ₄	330.50	4	3	97.54	2.36	0.55
20	Darutigenol	C ₂₀ H ₃₄ O ₃	322.50	3	3	94.14	3.05	0.55
21	Citrusin	C ₁₆ H ₂₂ O ₇	326.34	7	4	81.19	-0.54	0.55
22	Ingenol**	C ₂₀ H ₂₈ O ₅	348.40	5	4	93.22	1.17	0.55
23	14-Deoxyandrographolide	C ₂₀ H ₃₀ O ₄	334.40	4	2	94.05	2.81	0.55
24	Lagochilin	C ₂₀ H ₃₆ O ₅	356.50	5	4	97.20	1.51	0.55
25	Diethyl Phthalate	C ₂₄ H ₃₈ O ₄	390.60	4	0	116.30	5.24*	0.55
26	Gamma-mangostin	C ₂₃ H ₂₄ O ₆	396.40	6	4	115.52	1.98	0.55
27	Riboflavin	C ₁₇ H ₂₀ N ₄ O ₆	376.40	8	5	96.99	-0.54	0.55
28	Cratoxyarborenone E	C ₂₄ H ₂₆ O ₆	410.50	6	3	119.99	2.19	0.55
29	Cyanidin-3-O-alpha-arabinoside	C ₂₀ H ₁₉ O ₁₀	419.40	10	7*	102.33	-1.22	0.55
30	3-Epilupeol	C ₃₀ H ₅₀ O	426.70	1	1	135.14*	6.92*	0.55
31	Isovitexin	C ₂₁ H ₂₀ O ₁₀	432.40	10	7*	106.61	-2.02	0.55
32	Cyanidin-3-O-rhamnoside	C ₂₁ H ₂₁ O ₁₀	433.40	10	7*	107.13	-1.00	0.55
33	Quercetin-3-O-pentoside	C ₂₀ H ₁₈ O ₁₁	434.30	11*	7*	104.19	-2.06	0.17*
34	Avicularin	C ₂₀ H ₁₈ O ₁₁	434.30	11*	7*	104.19	-2.06	0.17*
35	Magnolol	C ₂₃ H ₂₈ O ₇	416.50	7	0	110.33	1.29	0.55
36	Betulin	C ₃₀ H ₅₀ O ₂	442.70	2	2	136.30*	6.00	0.55

Table 1. (Continue). The absorption parameters of *C. caudatus* compounds use the Lipinski rule of five and the drug-likeness parameter.

No	Compound	Physicochemical Properties					Lipophilicity	Drug-likeness
		Molecular Formula	MW (≤500)	nON (≤10)	nOHNH (≤5)	MR (40–130)	Log $P_{o/w}$ (≤5)	Bioavailability ≥ 30%
37	Quercitrin	C ₂₁ H ₂₀ O ₁₁	448.40	11*	7*	109.00	-1.84	0.17*
38	5-O-methylvisammioside	C ₂₄ H ₂₄ N ₂ O ₇	452.50	10	4	111.29	-1.43	0.55
39	Afzelin	C ₂₂ H ₁₆ N ₄ O ₆	432.40	10	6*	106.97	-1.34	0.55
40	Quercetin 3-O-alpha-L-Arabinopyranoside	C ₂₀ H ₁₈ O ₁₁	434.30	11*	7*	104.19	-2.06	0.17*
41	Peonidin-3-O-glucoside	C ₂₂ H ₂₃ O ₁₁	498.90	11*	7*	118.62	-1.33	0.17*
42	Isoquercitrin	C ₂₁ H ₂₀ O ₁₂	464.40	12*	8*	110.16	-2.59	0.17*
43	Hyperoside	C ₂₁ H ₂₀ O ₁₂	464.40	12*	8*	110.16	-2.59	0.17*
44	Homoorientin	C ₂₁ H ₂₀ O ₁₁	448.40	11*	8*	108.63	-2.51	0.17*
45	Oleanolic acid	C ₃₀ H ₄₈ O ₃	456.70	3	2	136.65*	5.82*	0.85
46	Glycyrrhetic acid	C ₃₀ H ₄₆ O ₄	470.70	4	2	136.85*	4.87	0.85
47	Quercetin-3-O-glucosyl-6'-acetate	C ₂₃ H ₂₂ O ₁₃	506.40*	13*	7*	119.89	-2.17	0.17*
48	3,4-di-O-caffeoylquinic acid	C ₂₅ H ₂₄ O ₁₂	516.40*	12*	7*	126.90	-0.35	0.11*
49	Ganoderic Acid A	C ₃₀ H ₄₄ O ₇	516.70*	7	3	141.05	2.26	0.56
50	Angeloylgomisin H	C ₂₇ H ₃₆ N ₂ O ₅ S	500.60*	8	1	138.03	2.45	0.55
51	Lappaconitine	C ₃₄ H ₄₀ N ₄ O ₅	584.70*	9	3	157.35	1.24	0.55
52	Rutin	C ₂₇ H ₃₀ O ₁₆	610.50*	16*	10*	141.38	-3.89	0.17*
53	Quercetin-3-O-rutinoside	C ₂₇ H ₃₀ O ₁₆	610.50*	16*	10*	141.38	-3.89	0.17*
54	Hirsutrin	C ₂₁ H ₂₀ O ₁₂	464.40	12*	8*	110.16	-2.59	0.17*
55	Coumaroyl Hexoside	C ₁₅ H ₁₈ O ₈	326.30	8	5	77.11	-1.12	0.55
56	Chlorogenic acid	C ₁₆ H ₁₈ O ₉	354.31	9	6*	83.50	-1.05	0.11*
57	Caffeoylquinic acid	C ₁₆ H ₁₈ O ₉	354.31	9	6*	83.50	-1.05	0.11*
58	Methyl chlorogenate**	C ₁₇ H ₂₀ O ₉	368.3	9	5	87.82	-0.81	0.55
59	Vitexin	C ₂₁ H ₂₀ O ₁₀	432.4	10	7*	106.61	-2.02	0.55
60	Kaempferol-3-O-rutinoside	C ₂₇ H ₃₀ O ₁₅	594.50*	15*	9*	139.36	-3.43	0.17*
61	Kaempferol-3-O-arabinoside	C ₂₀ H ₁₈ O ₁₀	418.30	10	6*	102.17	-1.57	0.55
62	Eriodictyol	C ₁₅ H ₁₂ O ₆	288.25	6	4	73.59	0.16	0.55
63	3',4',5,7-tetrahydroxyflavone	C ₁₅ H ₁₀ O ₆	286.24	6	4	76.01	-0.03	0.55
64	Quercetin	C ₁₅ H ₁₀ O ₇	302.23	7	5	78.03	-0.56	0.55
65	Rubiadin	C ₁₅ H ₁₀ O ₄	254.24	4	2	68.76	0.92	0.55
66	Apigenin	C ₁₅ H ₁₀ O ₅	270.20	5	3	73.99	0.52	0.55
67	Chrysoeriol	C ₁₆ H ₁₂ O ₆	300.26	6	3	80.48	0.22	0.55
68	Emodin	C ₁₅ H ₁₀ O ₅	270.24	5	3	70.78	0.36	0.55
69	Dinoseb	C ₁₀ H ₁₂ N ₂ O ₅	240.21	5	1	65.50	0.59	0.55
70	Aurapten	C ₁₉ H ₂₂ O ₃	298.40	3	0	91.29	3.51	0.55

Notes: *not eligible, **no target gene. MW (molecular weight), nON (H-bond acceptor), nOHNH (H-bond donor), and MR (molar refractivity).

3.3. Absorption parameters of chemical compounds

In this investigation, the Lipinski rules of five (MW, nON, nOHNH, MR, and miLogP) and drug-likeness were satisfied by 40 of the 70 active compounds found in *C. caudatus*. **Table 1** presents specific information about the compounds and screening parameter parameters. Most compounds that were screened utilizing Lipinski's rule of five did not match the requirements for molecular weight (MW), H-bond donors (nOHNH), and H-bond acceptors (nON).

3.4. Prediction and validation of chemical components' target

Swiss Target Prediction and SuperPred are used to examine further compounds that meet the Lipinski rule of five and drug-likeness parameters to determine their targets. Of the 40 compounds, 38 had targets, and two—ingenol and methyl chlorogenate—did not have any targets in the examined database. After the identical proteins were removed from the analysis, 230 target proteins were found. From them, 165 targets were found.

3.5. Disease and pathway screening of *Cosmos caudatus* compounds

Two hundred thirty diseases had been identified by disease screening using the Therapeutic Target Database (TTD) and the Comparative Toxicogenomics Database of targets. Because some targets matched the same disease as other targets, 91 diseases were found out of them. After removing the same pathway data and conducting a search applying disease data, 32 pathways were identified.

3.6. Network pharmacology

The compound, target, disease, and pathway data were then selected to build a general multi-compound–multi-target–multi-disease–multi-pathway network (**Figure 3**) with topological features for evaluation of the formed network interactions presented in **Tables 2-5** and cancer-specific networks (**Figure 4**), as well as breast neoplasms-specific networks (**Figure 5**) with topological features in **Tables 6-9**. The general pharmacology network resulted in 394 nodes and 742 edges. The cancer-specific network generated 138 and 169 nodes and edges, respectively, while the breast neoplasms network generated 41 nodes and 54 edges. We identified compounds and targets with the most degrees in the breast neoplasms-specific network, namely eriodictyol, cratoxyarborenone E, gamma-mangostin, isorhamnetin, bisdemethoxycurcumin each 3; and ABCC1 5 degrees; through the signal transduction pathway. The greater the number of degrees formed in the network, the greater the possibility of the compound, target, disease, and pathway being the key and primary mechanism in treating breast neoplasms from *C. caudatus*.

3.7. Protein-protein interaction network

In the protein-protein interaction network, nodes and edges, 40 and 229, respectively (**Figure 6**), were formed, with topological features detailed in **Table 10**. The three proteins with the highest degree, namely EGFR and NFKB1, as well as EP300 and H3-3B, were 30, 24, and 23, respectively. The nodes identified in the PPI network represent the linkages during the development of breast neoplasms.

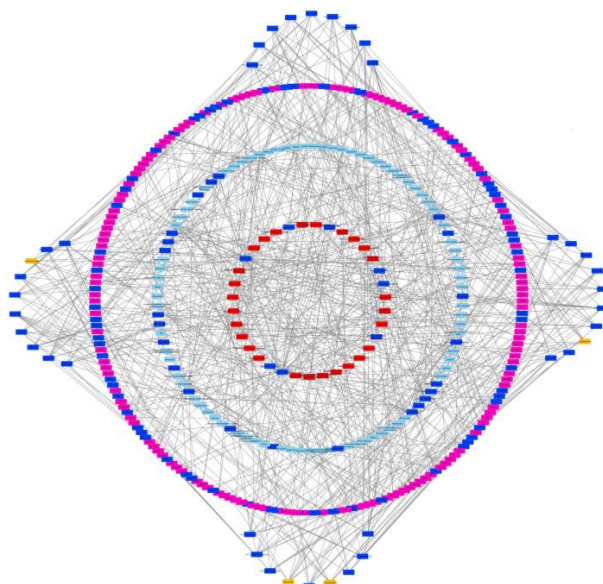


Figure 3. A graphic representation of the interaction between *C. caudatus*'s multiple compounds, multiple targets, multiple diseases, and multiple pathways using a pharmacological networking diagram. Yellow nodes represent the compound, a target is pink, a disease is light blue, and a disease pathway is red. The blue nodes in the network represent compounds, targets, diseases, and pathways associated with cancer.

Table 2. Topological features (betweenness centrality, closeness centrality, degree, indegree, outdegree) are all compounds in the network.

Compound	Betweenness Centrality	Closeness Centrality	Degree	Indegree	Outdegree
Auraptin	0	0.537037037	10	0	10
Dinoseb	0	0.530612245	10	0	10
Emodin	0	0.551020408	10	0	10
Chrysoeriol	0	0.545454545	10	0	10
Apigenin	0	0.538461538	10	0	10
Rubiadin	0	0.549019608	10	0	10
Quercetin	0	0.516666667	10	0	10
3',4',5,7-tetrahydroxyflavone	0	0.540000000	10	0	10
Eriodictyol	0	0.575000000	10	0	10
Coumaroyl Hexoside	0	0.500000000	10	0	10
5-O-methylvisammioside	0	0.517241379	10	0	10
Magnolin	0	0.594594595	10	0	10
Cratoxyarborenone E	0	0.589743590	10	0	10
Riboflavin	0	0.575000000	10	0	10
Gamma-mangostin	0	0.571428571	10	0	10
Lagochilin	0	0.538461538	10	0	10
14-Deoxyandrographolide	0	0.517241379	10	0	10
Citrusin	0	0.500000000	10	0	10
Darutigenol	0	0.492957746	10	0	10
Ceratodictyol	0	0.529411765	10	0	10
(S)-[6]gingerol	0	0.564102564	10	0	10
Isorhamnetin	0	0.545454545	10	0	10
Triptophenolide	0	0.555555556	10	0	10

Table 2. (Continue). Topological features (betweenness centrality, closeness centrality, degree, indegree, outdegree) are all compounds in the network.

Compound	Betweenness Centrality	Closeness Centrality	Degree	Indegree	Outdegree
Bisdemethoxycurcumin	0	0.578947368	10	0	10
Retinoic acid	0	0.589743590	10	0	10
Fallacinol	0	0.560000000	10	0	10
2'-Methoxyformonetin	0	0.547169811	10	0	10
Kaempferol	0	0.540000000	10	0	10
Luteolin	0	0.517857143	10	0	10
Piperine	0	0.500000000	10	0	10
Norambreinolide	0	0.487179487	10	0	10
Galaxolidone	0	0.528301887	10	0	10
Aloe-emodin	0	0.666666667	10	0	10
Atractylenolide III	0	0.520000000	10	0	10
Curcumenol	0	0.530612245	10	0	10
Muurolladie-3-One	0	0.568181818	10	0	10
Homononactinic acid	0	0.469135802	10	0	10
Humulene (alpha)	0	0.507936508	10	0	10

Table 3. Topological features (betweenness centrality, closeness centrality, degree, indegree, outdegree) all target network (top 10 based on degree value).

Target	Betweenness Centrality	Closeness Centrality	Degree	Indegree	Outdegree
CYP19A1	0.046572483	0.714285714	15	12	3
AKR1B1	0.030905841	0.600000000	10	9	1
CA7	0.009684399	0.666666667	8	7	1
MAOA	0.013719526	0.750000000	8	6	2
XDH	0.007655042	0.666666667	8	7	1
ADORA1	0.020926228	0.714285714	8	5	3
CA12	0.010524318	0.666666667	7	6	1
CA2	0.014782194	0.600000000	7	6	1
NOX4	0.012481079	0.666666667	7	6	1
FLT3	0.010651000	0.666666667	7	6	1

Table 4. Topological features (betweenness centrality, closeness centrality, degree, indegree, outdegree) all disease networks (top 10 based on degree value).

Disease	Betweenness Centrality	Closeness Centrality	Degree	Indegree	Outdegree
Breast Neoplasms	0.024313693	1	23	22	1
Necrosis	0.113620013	1	19	16	3
Inflammation	0.026310850	1	17	16	1
Chemical and Drug Induced Liver Injury	0.035830145	1	14	13	1
Prostatic Neoplasms	0.016426055	1	11	10	1
Weight Loss	0.042595047	1	10	8	2
Carcinoma, Hepatocellular	0.033161904	1	10	8	2
Prenatal Exposure Delayed Effects	0.012140210	1	7	6	1
Hypertension	0.006483473	1	7	6	1
Hyperplasia	0.004907926	1	6	5	1

Table 5. Topological features (betweenness centrality, closeness centrality, degree, indegree, outdegree) are all pathway networks (top 10 based on degree value).

Pathway	Betweenness Centrality	Closeness Centrality	Degree	Indegree	Outdegree
Signal Transduction	0	0	38	38	0
Immune System	0	0	25	25	0
Metabolism	0	0	14	14	0
Insulin Resistance	0.028432025	1	7	4	3
Cytokine-cytokine receptor interaction	0	0	3	3	0
Gene Expression	0	0	3	3	0
Adrenergic signaling in cardiomyocytes	0	0	3	3	0
Activation of gene expression by SREBF (SREBP)	0	0	3	3	0
Class A/1 (Rhodopsin-like receptors)	0	0	2	2	0
Basal cell carcinoma	0	0	2	2	0

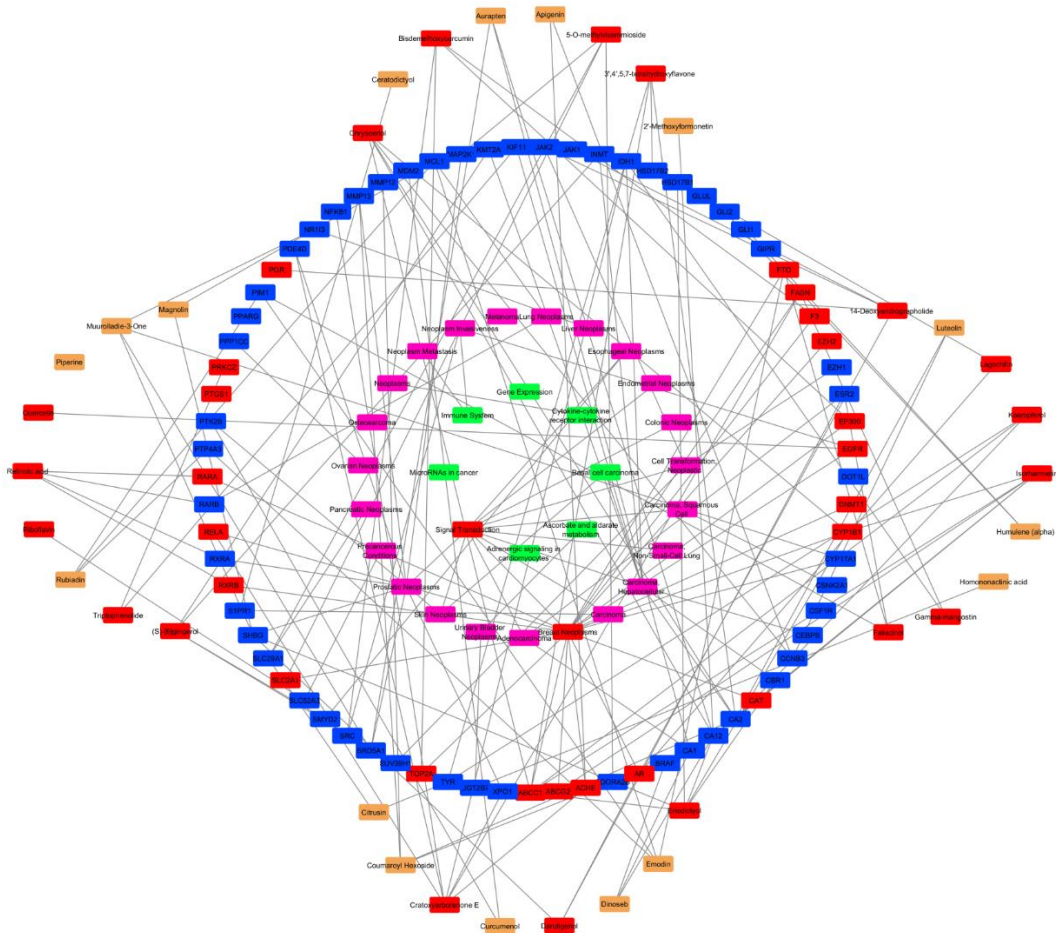


Figure 4. Pharmacological networks describing cancer-specific multi-compound–multi-target–multi-disease–multi-pathway interactions. Light brown nodes represent compounds, blue represents targets, pink represents disease, and blue represents disease pathways. Red nodes in the network system depict compounds, targets, diseases, and pathways associated with breast neoplasms.

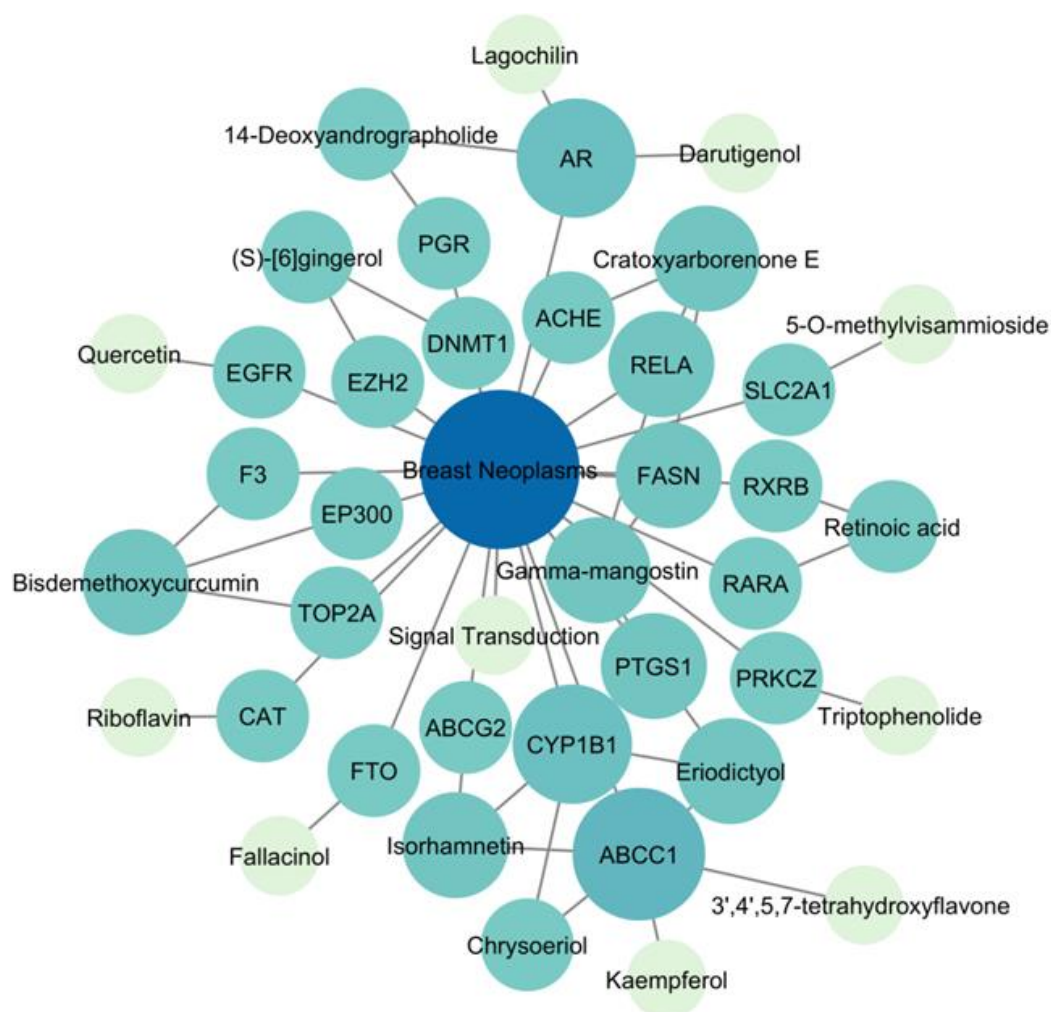


Figure 5. Connectivity between multiple compounds, targets, diseases, and pathways specific to breast neoplasms. The nodes' produced degree and the number of edges interacting with them are shown by the more significant and profound blue color developed on them.

Table 6. Topological features (betweenness centrality, closeness centrality, degree, indegree, outdegree) are all compound networks, especially of breast neoplasms (top 10 based on degree value).

Compound	Betweenness Centrality	Closeness Centrality	Degree	Indegree	Outdegree
Eriodictyol	0	0.625000000	3	0	3
Cratoxyarborenone E	0	0.625000000	3	0	3
Gamma-mangostin	0	0.625000000	3	0	3
Isorhamnetin	0	0.625000000	3	0	3
Bisdemethoxycurcumin	0	0.625000000	3	0	3
Chrysoeriol	0	0.571428571	2	0	2
14-Deoxyandrographolide	0	0.571428571	2	0	2
(S)-[6]gingerol	0	0.571428571	2	0	2
Retinoic acid	0	0.571428571	2	0	2
Quercetin	0	0.500000000	1	0	1

Table 7. Topological features (betweenness centrality, closeness centrality, degree, indegree, outdegree) all target networks, especially breast neoplasms (top 10 based on degree value).

Target	Betweenness Centrality	Closeness Centrality	Degree	Indegree	Outdegree
ABCC1	0.120940	0.666667	6	5	1
AR	0.044872	0.666667	4	3	1
CYP1B1	0.035043	0.666667	4	3	1
RELA	0.017094	0.666667	3	2	1
FASN	0.017094	0.666667	3	2	1
PTGS1	0.018803	0.666667	3	2	1
EGFR	0.038462	0.666667	2	1	1
SLC2A1	0.030769	0.666667	2	1	1
ACHE	0.009402	0.666667	2	1	1
CAT	0.025641	0.666667	2	1	1

Table 8. Topological features (betweenness centrality, closeness centrality, degree, indegree, outdegree) disease network, especially of breast neoplasms.

Disease	Betweenness Centrality	Closeness Centrality	Degree	Indegree	Outdegree
Breast Neoplasms	0.507051282	1	22	21	1

Table 9. Topological features (betweenness centrality, closeness centrality, degree, indegree, outdegree) pathway network especially of breast neoplasms.

Pathway	Betweenness Centrality	Closeness Centrality	Degree	Indegree	Outdegree
Signal Transduction	0	0	1	1	0

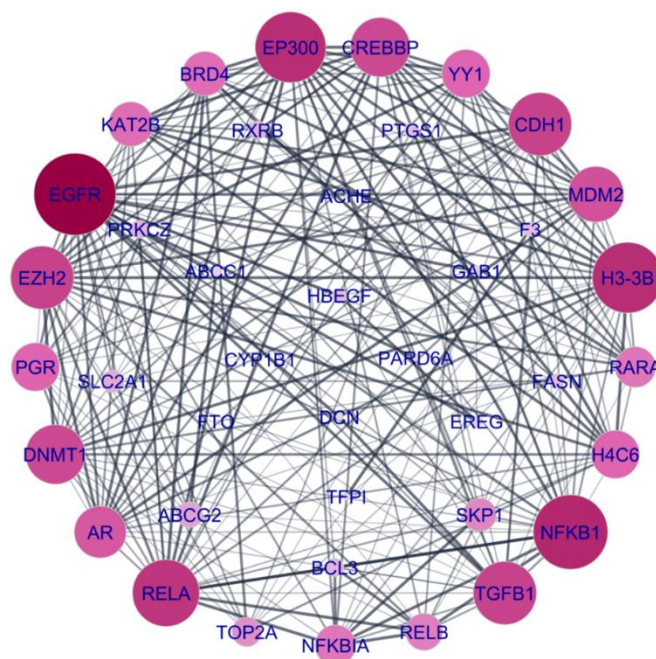


Figure 6. An overview of primary targets and breast neoplasms that create protein-protein interactions (PPIs). Larger nodes and a darker pink color show more interactions between more proteins.

Table 10. Topological features (betweenness centrality, closeness centrality, clustering coefficient, and degree) of protein-protein interaction (PPI) network analysis (top 10 based on degree value).

Display name	Betweenness Centrality	Closeness Centrality	Clustering Coefficient	Degree
EGFR	0.290751	0.812500	0.324138	30
NFKB1	0.062725	0.709091	0.514493	24
H3-3B	0.060866	0.696429	0.600791	23
EP300	0.037583	0.696429	0.600791	23
RELA	0.031155	0.672414	0.610390	22
EZH2	0.024274	0.672414	0.694737	20
CDH1	0.046416	0.661017	0.547368	20
TGFB1	0.088755	0.661017	0.473684	20
DNMT1	0.010744	0.650000	0.742690	19
CREBBP	0.016978	0.650000	0.713450	19

3.8. Gene ontology and the KEGG pathway

GO analysis of target genes using BP, CC, and MF parameters positively regulated NF-kappaB transcription factor activity, chromatin, and transcriptional coactivator binding. The KEGG pathway yielded pathways in cancer, microRNA in cancer, and chemical carcinogenesis-receptor activation as the top three pathways. This analysis was calculated using a p-value <0.01 and the Bonferroni method. The results of the top 15 GOs are presented in **Figure 7**.

3.9. Active component-main target of molecular docking molecular

By observing the compounds' two-dimensional (2-D) structures after docking with the target, 18 compounds that directly interact with the target were identified. Some compounds interact with the target through hydrogen bonding, and three compounds interact with the target without hydrogen bonding, namely kaempferol-4C3Z, fallacinol-7WCV, and eriodictyol-6IQ5. The lower the binding energy after docking, the more stable the conformation. The three compounds with the best binding energy are 5-O-methylvisammioside-SLC2A1 (6tha) ($-10.3 \text{ kcal mol}^{-1}$), isorhamnetin-CYP1B1 (6iq5) ($-10.1 \text{ kcal mol}^{-1}$), and eriodictyol-CYP1B1 (6IQ5) ($-10.0 \text{ kcal mol}^{-1}$). At this stage, the interaction between eriodictyol-CYP1B1 (6IQ5) has no hydrogen bonds, so the interaction of eriodictyol-5UHP ($-9.0 \text{ kcal mol}^{-1}$) is the best alternative. The binding affinities and amino acid residues are detailed in **Table 11**. The ligand-receptor interactions of the three complexes with the most hydrogen bonds were identified on 5-O-methylvisammioside-6THA, namely, Trp412, Ser80, and Asn288. Part of the docking results (3-D and 2-D) are shown in **Figure 8a-c**.

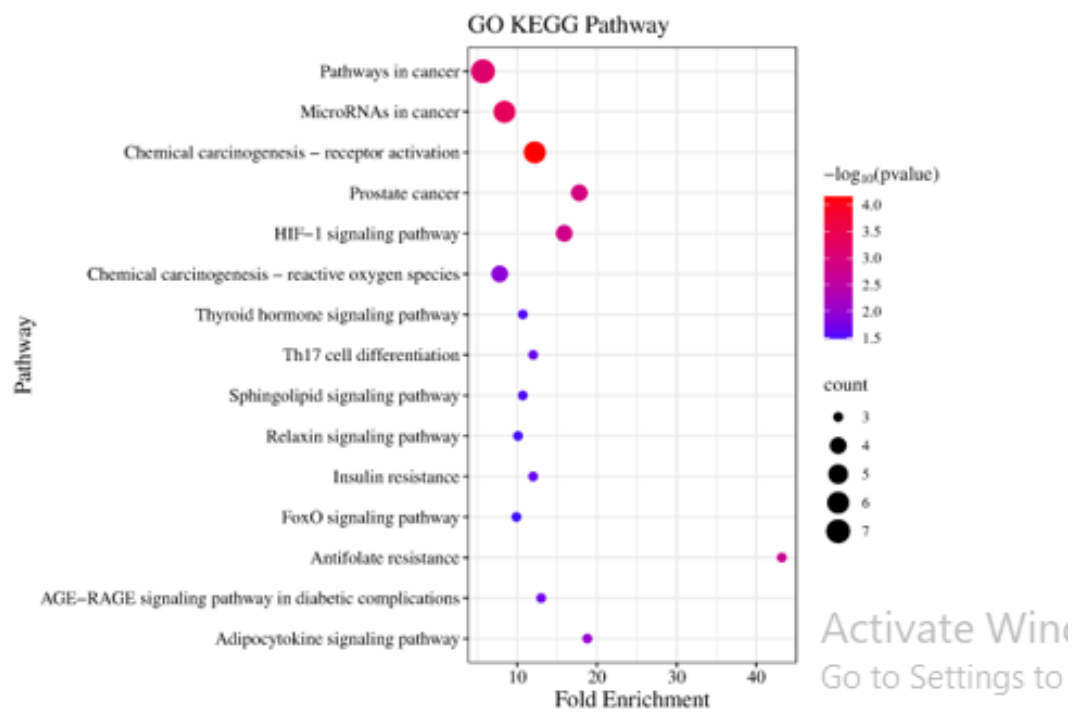
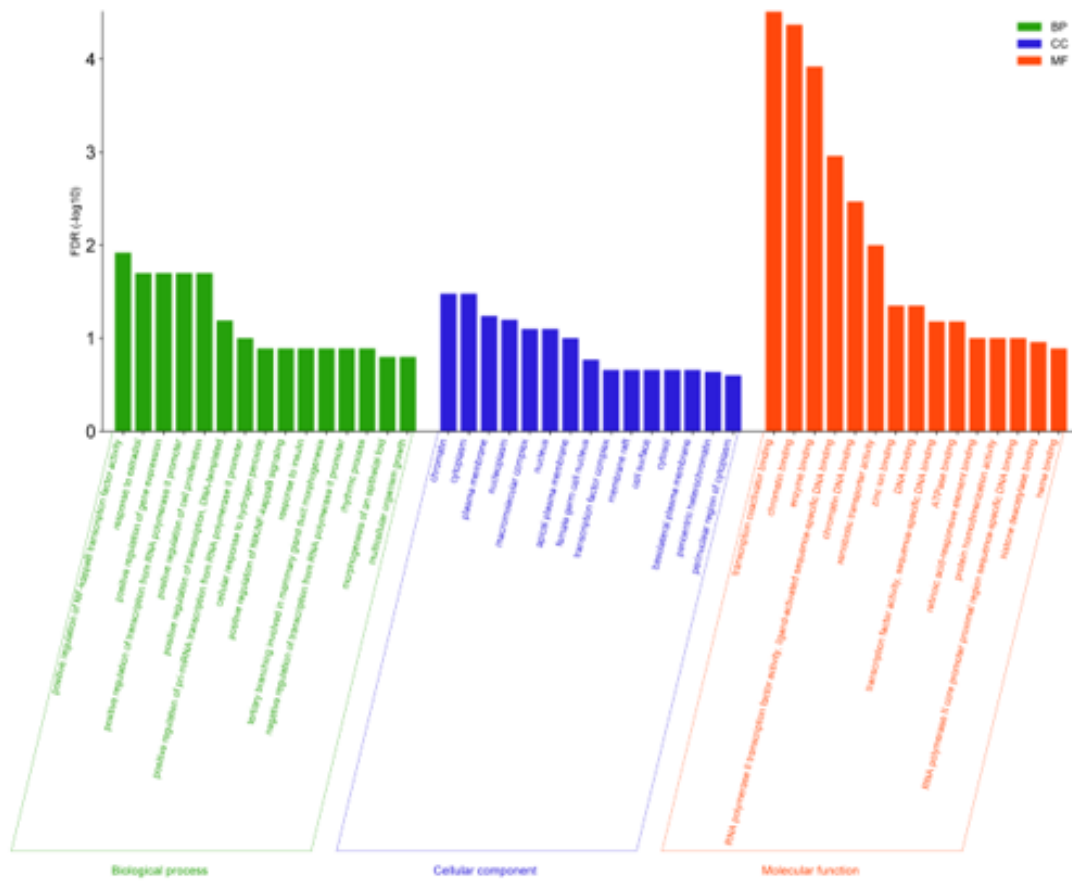


Figure 7. Gene ontology (GO) terms for cellular component (CC), molecular function (MF), biological process (BP), and KEGG pathway direct top 15, respectively, are associated with breast neoplasms.

Table 11. Ligand, receptor target, binding affinity, and amino acid residues of computational docking on the active site of *Cosmos caudatus* compounds. Bold letters indicate hydrogen bonds.

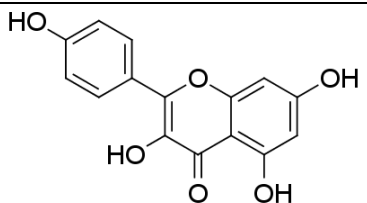
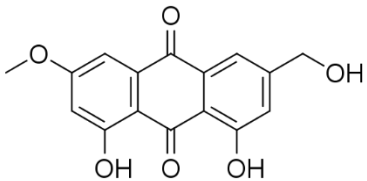
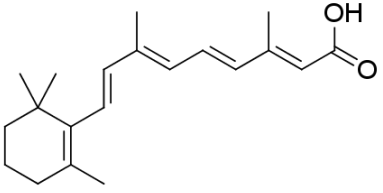
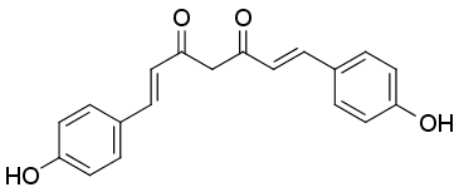
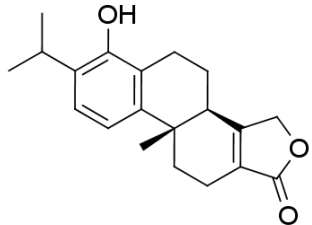
No	Ligand (PubChem ID)	Structure	Recept or (PDB ID)	Binding Affinity Kcal mol ⁻¹	AA Residue
1	Kaempferol (5280863)		4C3Z	-7.0	Ser871, Ser796, Asp793, Leu824, Leu795, Pro794, Ile811, Phe807, Thr826, Tyr831, ser828, Ser830
2	Fallacinol (3083633)		7WCV	-8.1	Arg322, His231, Leu109, Ser229, Ile85, His232, Glu234, Asp233, Tyr106
3	Retinoic acid (444795)		8J2P	-8.9	Tyr-35, Phe-34, Trp40, Ala-127, Trp-128, Trp150, Met140, Arg-124 , Arg154
			5HJP	-7.2	Pro352, Lys452, Val434, Glu355, Asp450, Arg362, Ala359, Pro457, Pro449, Asn351
4	Bisdemethoxycurcumin (5315472)		5UYS	-6.7	Lys222, Leu229, Leu221, Phe224, Asn226, Thr228 , Lys227 , Pro225, Lys211, Asp212 , Ile479, Lys481, Glu230
			6WJ7	-7.7	Leu70, His104 , Trp124, Gly103 , Ile131, Gly71, Gln72, Leu73, His99 , Tyr69, Gln100 , His109, Thr106 , His109 , Glu108, Pro102,
			7SMD	-6.2	Lys553 , Asp805 , Arg802, Pro872
5	Triptophan nolide (173273)		4MJS	-7.5	Gly24 , Ile99, Gly23 , Glu14, Asp15, Phe96, Ala16

Table 11. (Continue). Ligand, receptor target, binding affinity, and amino acid residues of computational docking on the active site of *Cosmos caudatus* compounds. Bold letters indicate hydrogen bonds.

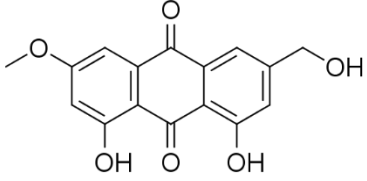
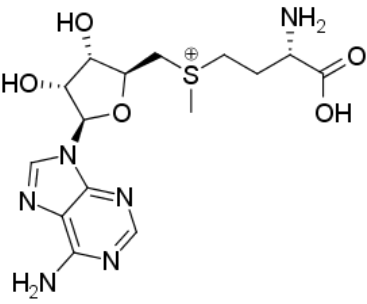
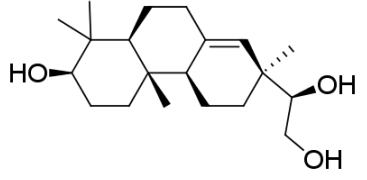
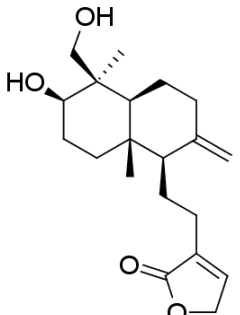
No	Ligand (PubChem ID)	Structure	Recept or (PDB ID)	Binding Affinity Kcal mol ⁻¹	AA Residue
6	Isorhamne tin (5281654)		6IQ5	-10.1	Asp326, Gly329, Phe231, Gln332, Asn228, Asp333, Asn265, Thr325, Val126, Ser131, Ser127 , Ala330, Ile390, Ala133
			4C3Z	-6.9	Leu795, Pro794, Tyr831 , Gly803, Ala800
			8BHT	-8.9	Val546, Phe439, Thr435, Met549, Phe439, Phe432 , Thr435 , Asn436
7	(S)- [6]gingero l (34756)		3PTA	-8.2	Trp1170, Phe1145, Glu1168 , Gly1147, Gly1223, Ala1579, Arg1312, Glu1266, Pro1224, Val1268, Asp700 , Asn1267 , Glu698 , Ala699, Asn1578 , Pro1225, Met1169
			5KJH	-7.9	Leu804, His881 , Tyr918, Arg2536, Arg877 , Tyr878, Ile879, Asn880 , Cys807, Val853, Tyr809, Tyr855, Pro302 , Lys927 , Leu925
8	Darutigen ol (3037565)		5UYS	-8.6	Phe172, Phe169, Glu305 , Ile206, Leu485
			5UHP	-9.0	Tyr569, Trp660, Phe657, Leu585 , Arg586 , Phe681
9	14- Deoxyand rographoli de (11624161)		5SKJ	-8.7	Phe729, Ile692, Leu675, Thr633 , His525, Asp674, Leu635, Gln726 , Tyr524
			5UHP	-8.3	Arg290, Phe681, Trp660, Phe657, Tyr569, Pro694, Pro568

Table 11. (Continue). Ligand, receptor target, binding affinity, and amino acid residues of computational docking on the active site of *Cosmos caudatus* compounds. Bold letters indicate hydrogen bonds.

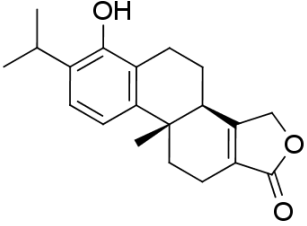
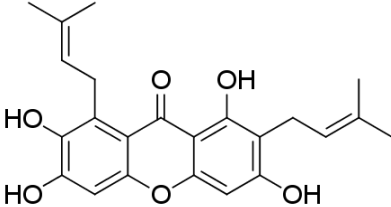
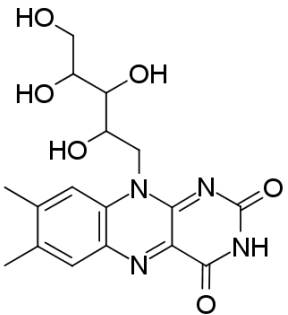
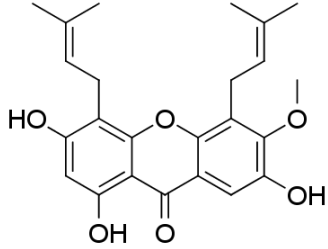
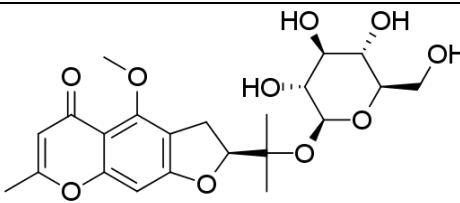
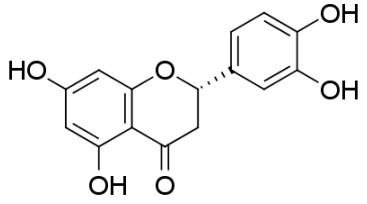
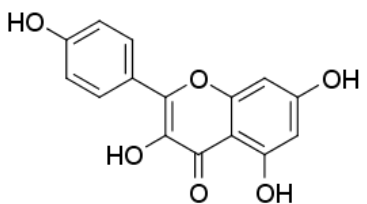
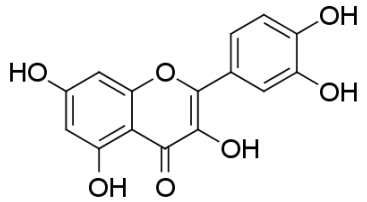
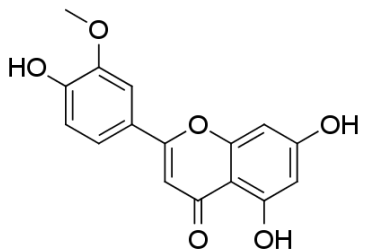
No	Ligand (PubChem ID)	Structure	Recept or (PDB ID)	Bindin g Affinit y Kcal mol ⁻¹	AA Residue
10	Lagochilin (7061097)		5UHP	-7.4	His571, Pro568, Arg290, Phe681 , Glu677, Trp660, Phe657, Leu585, Arg586 , Tyr569
11	Gamma- mangostin (5464078)		6Y3C	-8.2	His388, His207, Val447, Val291, Leu294, Leu408, Gln203 , Ala202, Tyr385 , Thr206
			4XJV	-8.1	Ala130, Thr131 , Gln151, Tyr155, His139, Leu184, Ile141, Pro142, Met35, Glu158, Met102, Val187, Tyr105
			2VGE	-7.4	Glu639, Ala634, Val642, Lys619 , Gln645, Ala646, Leu630, Arg621, Pro627
12	Riboflavin (493570)		4E9E	-6.5	Tyr540, Leu466, Gly471, Ser470, Lys562, Asp560 , Thr469, Arg468 , Asn467
13	Cratoxyar borenone E (5323543)		4VGE	-6.4	Pro811, Trp798, Gly727, Thr722, Thr729, Phe720, Asp797 , Asn813 , Arg812
			4XJV	-7.6	Leu184, Val187, Ile141, Tyr155, His154, His139, Thr131 , Ile213
			6U3P	-8.8	Ser293 , Leu289, Trp286, Arg296 , Phe295 , Phe338, Tyr341, Tyr124, Asp74, Leu76, Tyr72

Table 11. (Continue). Ligand, receptor target, binding affinity, and amino acid residues of computational docking on the active site of *Cosmos caudatus* compounds. Bold letters indicate hydrogen bonds.

No	Ligand (PubChem ID)	Structure	Recept or (PDB ID)	Binding Affinity Kcal mol ⁻¹	AA Residue
14	5-O-methylvisammioside (21670038)		6THA	-10.3	Ile404, Gly408, Trp412 , Ser80 , Thr137, Trp388, Tyr292, Gln283, Asn288 , His160
15	Eriodictyol (440735)		6IQ5	-10.0	Asp326, Phe134, Val126, Leu264, Asn228, Phe268, Phe231, Ala133, Ile399, Ala330
			6Y3C	-8.3	His207 , Lys211, Thr212 , Tyr148, Asn382 , Phe210, His386, Tyr385, Thr206 , His388, Ala202, Gln203
			4C3Z	-7.2	Ser828, Ser796, Ser830, Asp793, Leu795, Pro794, Ala800 , Lys804
16	3',4',5,7-tetrahydroxyflavone (5280863)		4C3Z	-7.0	Phe807, Tyr831 , Lys804, Val798, Ala800, Ser796, Pro794, Leu795, Asp793, Val825
17	Quercetin (5280343)		3GKW	-7.8	Pro41, Gln43, Gly42 , Thr85 , Gln38 , Thr39, Gly41, Lys42, Gln39, Trp103, Ala88, Phe89
18	Chrysoeriol (5280666)		4C3Z	-7.3	Val798, Tyr831 , Phe807, Val825, Asp793, Pro794, Leu795, Ser796, Ala800
			6IQ5	-8.4	Glu474 , Ala186, Arg469 , Val460 , Arg459 , Lys477 , Glu473

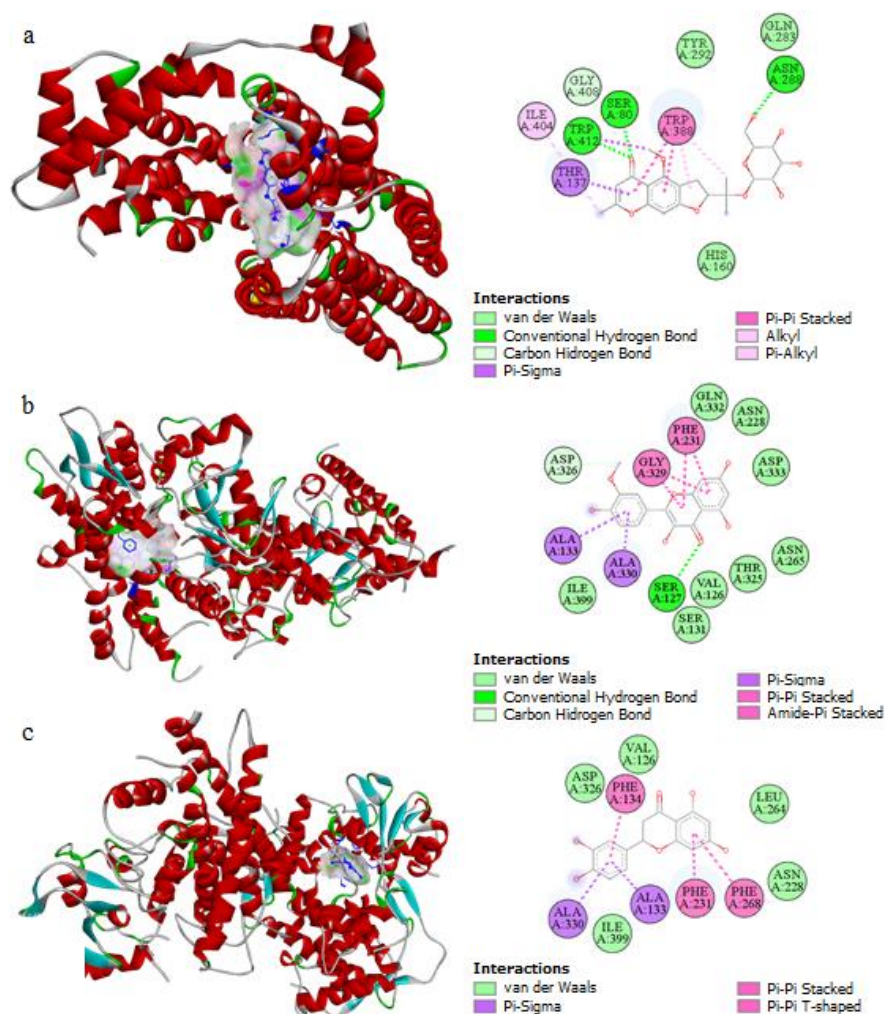


Figure 8. Molecular docking of the core compound-target pair of *C. caudatus* treatment for breast neoplasm (3-D and 2-D visualization). Core compounds and receptor proteins: (a) 5-methylvisammioside–6THA, (b) isorhamnetin–6IQ5, and (c) eriodictyol–6IQ5.

3.10. Discussion

This study reported 70 active compounds identified in *C. caudatus*. After screening, 40 active compounds were identified as having good ADME ability and drug-likeness. This parameter profile (applied as a preliminary evaluation of the drug properties of natural materials) can increase the success rate of drugs, save drug development costs, reduce side effects and drug toxicity, and further guide the rational clinical use of drugs and confirm the possibility of these compounds becoming drug candidates in the treatment of breast neoplasms (Olowosoke *et al.*, 2024; Syahrani *et al.*, 2023; Tabti *et al.*, 2024). The most common route of drug delivery is the oral route; this route is widely applied in both local and systemic treatment, in addition to its advantages such as the convenience of drug administration, cost-effectiveness, and ease of manufacturing large-scale oral dosage forms (Alqahtani *et al.*, 2021; Lou *et al.*, 2023).

The network generally shows the targets, diseases, and pathways with the highest degree of CYP19A1, breast neoplasms, and signal transduction, respectively. Degree in the network shows the number of targets associated with nodes based on topological analysis; the more degree values indicated, the more critical the component or target is (Cao *et al.*, 2024; Sun *et*

al., 2024). Specifically in the breast neoplasms disease-specific network, the highest degree of compounds, targets, diseases, and pathways are eriodictyol, cratoxyarborenone E, gamma-mangostin, isorhamnetin, and bisdemethoxycurcumin; ABCC1; breast neoplasms; and signal transduction, respectively.

Eriodictyol was reported to suppress tumor growth, inhibit mitochondrial dysfunction, and downregulate Nrf2 (NF-E2-related factor-2) in tumor tissues (Deng et al., 2020; Islam et al., 2020), besides regulating ferroptosis and cell survival through Nrf2/HO-1/NQO1 signaling pathway in ovarian cancer (Wang et al., 2023). Decreased Nrf2 expression in breast cancer can degrade autophagic Keap1 (Shirvanian et al., 2024; Xue et al., 2024). Cratoxyarborenone E, a xanthenes compound, may have effects against breast cancer, as this compound has been reported to have toxic properties on the human oral epidermoid carcinoma (KB) cell line (Yin Bok et al., 2023). Gamma-mangosteen and alpha-mangosteen inhibit breast cancer cell migration and induce cellular ROS levels in MDA-MB-231 cells; in particular, γ -mangosteen suppresses CXCR4 mRNA expression which may correlate with its activity in inhibiting MDA-MB-231 cell migration (Sarmoko et al., 2023), as well as inducing apoptosis and inhibiting metastasis of breast cancer through regulation of the RXR α -AKT Signaling Pathway (Zhu et al., 2021), besides that this compound is also reported to have anticancer activity and induce apoptosis in HT29 colorectal adenocarcinoma cells (Chang & Yang, 2012). Isorhamnetin exhibits antitumor effects in breast cancer, which are mediated by Akt and MEK signaling pathways (Hu et al., 2015), potent cytotoxic effects via ROS-dependent apoptotic pathway in MCF-7 cells (Wu et al., 2018), inhibits MDA-MB-231 cell invasion by decreasing the expression and activity of MMP-2 and MMP-9, potentially related to suppression of p38 MAPK and STAT3 (Li et al., 2015). Isorhamnetin was also reported to inhibit the EGFR-STAT3-PD-L1 signaling pathway and block cancer growth, significantly increasing the survival rate of healthy cells. The cell membrane receptor EGFR was identified as a direct target of isorhamnetin (Mei et al., 2024). Bisdemethoxycurcumin decreased breast cancer (MDA-MB-231) cell viability (Huang et al., 2020), effectively suppressed GPR161-mediated TNBC (triple negative breast cancer) metastasis through inhibiting Twist1/MMP9-induced EMT (epithelial-mesenchymal transition) (Chou et al., 2021). The multidrug resistance-associated protein 1 (MRP1) encoded by the ABCC1 gene is one of the most studied ABC (ATP-binding cassette) subfamily C transporters. ABCC1, in general, leads to cell proliferation, so by inhibiting ABCC1, cell proliferation will be inhibited (He et al., 2021; Kunická & Souček, 2014; Nedeljković et al., 2021).

The resulting protein-protein interactions result in the highest levels of EGFR and NFKB1. The amount of EGFR (the epidermal growth factor receptor) overexpression determines the degree of dysregulation of its natural functions (regulation of cell proliferation, differentiation, migration, and survival), and its use as an indicator of clinical outcome has been reported in several tumor types, including breast cancer (Hermawan et al., 2024; Maennling et al., 2019; Wang et al., 2024). The NFKB1 signaling pathway is one of the most important links between inflammation and tumorigenesis. NFKB1 is a superfamily of transcription factors that play important roles in several types of hematological and solid tumors, including breast cancer (Concetti & Wilson, 2018; Espinoza-Sánchez et al., 2019; Kim et al., 2016).

In this study, gene ontology in biological processes (BP) showed positive NF-kappaB transcription factor activity regulation. The NF-KB signaling pathway is one of the most important links between inflammation and tumorigenesis. NF-KB is a superfamily of transcription factors that play an essential role in several types of tumors, including breast cancer. The NF-KB family has been described as an important regulator of many biological

processes, including cell proliferation, differentiation, immune response, and inflammation. The family consists of five subunits: p50 (NF-KB1), p52 (NF-KB2), p65 (RelA), c-Rel (Rel), and RelB, which combine to form functional homo- and heterodimers (Jin *et al.*, 2024; Pires *et al.*, 2017). CC (cellular component) chromatin is a macromolecular structure composed of DNA and histone proteins, which play an important role in transcription factors, signaling pathways, and other signals altering gene activity and cellular phenotypes. DNA and histone proteins are modified to regulate accessibility and function, and changes in these modifications are one of the hallmarks of cancer (Kim *et al.*, 2024; Tao *et al.*, 2024). MF (transcription coactivator binding), activation of transcription factors promotes the transcription of genes associated with tumor proliferation, metastasis, and suppression of apoptosis (Ren *et al.*, 2024). KEGG analysis reveals pathways in cancer and microRNAs in cancer. MicroRNA (miRNA) is important in gene regulation and biological processes. MiRNAs can be differentially expressed in normal and malignant tissues, possibly regulating tumor progression, invasion, and metastasis in cancer (Martino *et al.*, 2024; Tluli *et al.*, 2023).

Molecular docking is a computational technique used to reveal interactions between components (ligands) and targets (receptors) in a network, thereby increasing the accuracy of the network. The compounds 5-O-methylvisammioside, isorhamnetin, and eriodictyol interact with SLC2A1 and CYP1B1 through several types of bonds, including hydrogen bonds. The strength and weakness of the binding affinity of the ligand to the receptor are greatly influenced by hydrogen bonds (Chen *et al.*, 2016; Itoh *et al.*, 2019). Solute carrier family 2 (facilitated glucose transporter) member 1 (SLC2A1) protein, also known as glucose transporter type 1 (GLUT1), is associated with tumor progression and metastasis. In breast cancer, SLC2A1 expression is closely correlated with tumor grade, contributing to carcinogenesis and higher tumor progression (Cha *et al.*, 2018; Wellberg *et al.*, 2016; Yan *et al.*, 2015). Cytochrome P450 1B1 (CYP1B1) catalyzes the metabolism of estrogen to produce metabolites that promote the development of breast cancer. By inhibiting CYP1B1, the development of breast cancer will be inhibited (Kwon *et al.*, 2024; Zheng *et al.*, 2024).

4. CONCLUSION

In summary, the pharmacological network shows that the main active components of *C. caudatus*, especially eriodictyol, cratoxyarborenone E, gamma-mangostin, isorhamnetin, and bisdemethoxycurcumin can act on multiple targets. *C. caudatus* compounds affect treating breast neoplasms, primarily through the signal transduction pathway in cancer. Molecular docking showed that 5-O-methylvisammioside, isorhamnetin, and darutigenol were the top three compounds, indicating that they may play an important role in treating breast neoplasms. However, the findings in this study are only based on computer simulations that need to be demonstrated through experimental protocols.

5. AUTHORS' NOTE

The authors declare that there is no conflict of interest regarding the publication of this article. Authors confirmed that the paper was free of plagiarism.

6. AVAILABILITY OF DATA AND MATERIALS

The datasets analyzed during the current study are available from Abdul Halim Umar (corresponding author) upon request.

7. REFERENCES

- Afendi, F. M., Okada, T., Yamazaki, M., Hirai-Morita, A., Nakamura, Y., Nakamura, K., Ikeda, S., Takahashi, H., Altaf-Ul-Amin, Md., Darusman, L. K., Saito, K., and Kanaya, S. (2012). KNApSACK family databases: Integrated metabolite–plant species databases for multifaceted plant research. *Plant and Cell Physiology*, 53(2), e1.
- Ahda, M., Jaswir, I., Khatib, A., Ahmed, Q. U., and Syed Mohamad, S. N. A. (2023). A review on *Cosmos caudatus* as a potential medicinal plant based on pharmacognosy, phytochemistry, and pharmacological activities. *International Journal of Food Properties*, 26(1), 344–358.
- Al Husaeni, D. F., and Nandiyanto, A. B. D. (2022). Bibliometric using VOSviewer with Publish or Perish (using google scholar data): From step-by-step processing for users to the practical examples in the analysis of digital learning articles in pre and post covid-19 pandemic. *ASEAN Journal of Science and Engineering*, 2(1), 19–46.
- Alqahtani, M. S., Kazi, M., Alsenaidy, M. A., and Ahmad, M. Z. (2021). Advances in oral drug delivery. *Frontiers in Pharmacology*, 12, 618411.
- Burley, S. K., Berman, H. M., Kleywegt, G. J., Markley, J. L., Nakamura, H., and Velankar, S. (2017). Protein Data Bank (PDB): The single global macromolecular structure archive. *Methods in Molecular Biology*, 1607, 627–641.
- Cao, M., Zhan, M., Jing, H., Wang, Z., Wang, Y., Li, X., and Miao, M. (2024). Network pharmacology and experimental evidence: MAPK signaling pathway is involved in the anti-asthma roles of *Perilla frutescens* leaf. *Heliyon*, 10(1), e22971.
- Cha, Y. J., Kim, E.-S., and Koo, J. S. (2018). Amino acid transporters and glutamine metabolism in breast cancer. *International Journal of Molecular Sciences*, 19(3), 907.
- Chang, H.-F., and Yang, L.-L. (2012). Gamma-mangostin, a micronutrient of mangosteen fruit, induces apoptosis in human colon cancer cells. *Molecules*, 17(7), 8010–8021.
- Chen, D., Oezguen, N., Urvil, P., Ferguson, C., Dann, S. M., and Savidge, T. C. (2016). Regulation of protein-ligand binding affinity by hydrogen bond pairing. *Science Advances*, 2(3), e1501240.
- Chen, T., Lei, Y., Li, M., Liu, X., Zhang, L., Cai, F., Gong, X., and Zhang, R. (2024). Network pharmacology to unveil the mechanism of suanzaoren decoction in the treatment of alzheimer's with diabetes. *Hereditas*, 161(1), 2.
- Chen, X., Ji, Z. L., and Chen, Y. Z. (2002). TTD: Therapeutic target database. *Nucleic Acids Research*, 30(1), 412–415.
- Cheng, S.-H., Barakatun-Nisak, M. Y., Anthony, J., and Ismail, A. (2015). Potential medicinal benefits of *Cosmos caudatus* (Ulam Raja): A scoping review. *Journal of Research in Medical Sciences: The Official Journal of Isfahan University of Medical Sciences*, 20(10), 1000–1006.
- Chou, C.-H., Wang, H.-K., Lin, Y.-C., Tsai, D.-H., Lu, M.-T., Ho, C.-T., Hseu, Y.-C., Yang, H.-L., and Way, T.-D. (2021). Bisdemethoxycurcumin promotes apoptosis and inhibits the epithelial–mesenchymal transition through the inhibition of the G-protein-coupled

- receptor 161/mammalian target of rapamycin signaling pathway in triple negative breast cancer cells. *Journal of Agricultural and Food Chemistry*, 69(48), 14557–14567.
- Concetti, J., and Wilson, C. L. (2018). NFKB1 and cancer: Friend or foe? *Cells*, 7(9), 133.
- Daina, A., Michielin, O., and Zoete, V. (2019). SwissTargetPrediction: Updated data and new features for efficient prediction of protein targets of small molecules. *Nucleic Acids Research*, 47(W1), W357–W364.
- Davis, A. P., Wieggers, T. C., Johnson, R. J., Sciaky, D., Wieggers, J., and Mattingly, C. J. (2023). Comparative Toxicogenomics Database (CTD): Update 2023. *Nucleic Acids Research*, 51(D1), D1257–D1262.
- Demir, G., Chatterjee, P., and Pamucar, D. (2024). Sensitivity analysis in multi-criteria decision making: A state-of-the-art research perspective using bibliometric analysis. *Expert Systems with Applications*, 237, 121660.
- Deng, Z., Hassan, S., Rafiq, M., Li, H., He, Y., Cai, Y., Kang, X., Liu, Z., and Yan, T. (2020). Pharmacological activity of eriodictyol: The major natural polyphenolic flavanone. *Evidence-Based Complementary and Alternative Medicine*, 2020, e6681352.
- Ellili, N. O. D. (2024). Bibliometric analysis of sustainability papers: Evidence from Environment, Development and sustainability. *Environment, Development and Sustainability*, 26(4), 8183–8209.
- Espinoza-Sánchez, N. A., Györfy, B., Fuentes-Pananá, E. M., and Götte, M. (2019). Differential impact of classical and non-canonical NF-κB pathway-related gene expression on the survival of breast cancer patients. *Journal of Cancer*, 10(21), 5191–5211.
- Firdaus, M. D., Artanti, N., Hanafi, M., and Rosmalena, R. (2021). Phytochemical constituents and in vitro antidiabetic and antioxidant properties of various extracts of kenikir (*Cosmos caudatus*) leaves. *Pharmacognosy Journal*, 13(4), 890–895.
- Goodsell, D. S., Zardecki, C., Di Costanzo, L., Duarte, J. M., Hudson, B. P., Persikova, I., Segura, J., Shao, C., Voigt, M., Westbrook, J. D., Young, J. Y., and Burley, S. K. (2020). RCSB Protein Data Bank: Enabling biomedical research and drug discovery. *Protein Science: A Publication of the Protein Society*, 29(1), 52–65.
- He, J., Fortunati, E., Liu, D.-X., and Li, Y. (2021). Pleiotropic roles of ABC transporters in breast cancer. *International Journal of Molecular Sciences*, 22(6), 3199.
- Herlina, H., Amriani, A., Sari, I. P., and Apriani, E. F. (2021). Acute toxicity test of kenikir leaf (*Cosmos caudatus* H.B.K) ethanolic extract on Wistar white male rats with fixed dose procedure method and its effect on histopathology of pancreatic cells. *Journal of Advanced Pharmaceutical Technology and Research*, 12(2), 157–161.
- Hermawan, A., Satria, D., Hasibuan, P. A. Z., Huda, F., Tafrihan, A. S., Fatimah, N., and Putri, D. D. P. (2024). Identification of potential target genes of cardiac glycosides from *Vernonia amygdalina* Delile in HER2+ breast cancer cells. *South African Journal of Botany*, 164, 401–418.

- Hu, S., Huang, L., Meng, L., Sun, H., Zhang, W., and Xu, Y. (2015). Isorhamnetin inhibits cell proliferation and induces apoptosis in breast cancer via Akt and mitogen-activated protein kinase signaling pathways. *Molecular Medicine Reports*, 12(5), 6745–6751.
- Huang, C., Lu, H.-F., Chen, Y.-H., Chen, J.-C., Chou, W.-H., and Huang, H.-C. (2020). Curcumin, demethoxycurcumin, and bisdemethoxycurcumin induced caspase-dependent and – independent apoptosis via Smad or Akt signaling pathways in HOS cells. *BMC Complementary Medicine and Therapies*, 20(1), 68.
- Huang, J., Xu, Z., Li, J., He, X., Huang, X., Shen, X., and Luo, Z. (2024). Systems pharmacology-based dissection of potential mechanisms of exocarpium *Citri grandis* for the treatment of chronic bronchitis. *Arabian Journal of Chemistry*, 17(1), 105428.
- Husain, S. S., Kadhim, M. Q., Al-Obaidi, A. S. M., Hasan, A. F., Humaidi, A. J., and Husaeni, D. N. A. (2023). Design of robust control for vehicle steer-by-wire system. *Indonesian Journal of Science and Technology*, 8(2), 197–216.
- Islam, A., Islam, M. S., Rahman, M. K., Uddin, M. N., and Akanda, M. R. (2020). The pharmacological and biological roles of eriodictyol. *Archives of Pharmacal Research*, 43(6), 582–592.
- Itoh, Y., Nakashima, Y., Tsukamoto, S., Kurohara, T., Suzuki, M., Sakae, Y., Oda, M., Okamoto, Y., and Suzuki, T. (2019). N⁺-C-H...O Hydrogen bonds in protein-ligand complexes. *Scientific Reports*, 9(1), 767.
- Jin, Q., Feng, J., Yan, Y., and Kuang, Y. (2024). Prognostic and immunological role of adaptor related protein complex 3 subunit mu2 in colon cancer. *Scientific Reports*, 14(1), 483.
- Kanehisa, M., and Goto, S. (2000). KEGG: Kyoto Encyclopedia of Genes and Genomes. *Nucleic Acids Research*, 28(1), 27–30.
- Kim, J., Kim, J., and Park, M. (2024). Synthetic interventions in epigenome: Unraveling chromatin's potential for therapeutic applications. *Current Opinion in Systems Biology*, 37, 100504.
- Kim, J.-Y., Jung, H. H., Ahn, S., Bae, S., Lee, S. K., Kim, S. W., Lee, J. E., Nam, S. J., Ahn, J. S., Im, Y.-H., and Park, Y. H. (2016). The relationship between nuclear factor (NF)- κ B family gene expression and prognosis in triple-negative breast cancer (TNBC) patients receiving adjuvant doxorubicin treatment. *Scientific Reports*, 6(1), 31804.
- Kim, S., Chen, J., Cheng, T., Gindulyte, A., He, J., He, S., Li, Q., Shoemaker, B. A., Thiessen, P. A., Yu, B., Zaslavsky, L., Zhang, J., and Bolton, E. E. (2021). PubChem in 2021: New data content and improved web interfaces. *Nucleic Acids Research*, 49(D1), D1388–D1395.
- Kim, S., Thiessen, P. A., Bolton, E. E., Chen, J., Fu, G., Gindulyte, A., Han, L., He, J., He, S., Shoemaker, B. A., Wang, J., Yu, B., Zhang, J., and Bryant, S. H. (2016). PubChem substance and compound databases. *Nucleic Acids Research*, 44(D1), D1202–D1213.
- Kunická, T., and Souček, P. (2014). Importance of ABCC1 for cancer therapy and prognosis. *Drug Metabolism Reviews*, 46(3), 325–342.
- Kwon, Y.-J., Kwon, T.-U., Shin, S., Lee, B., Lee, H., Park, H., Kim, D., Moon, A., and Chun, Y.-J. (2024). Enhancing the invasive traits of breast cancers by CYP1B1 via regulation of p53 to

- promote uPAR expression. *Biochimica et Biophysica Acta (BBA) - Molecular Basis of Disease*, 1870(1), 166868.
- Lee, T. K., and Vairappan, C. S. (2011). Antioxidant, antibacterial and cytotoxic activities of essential oils and ethanol extracts of selected South East Asian herbs. *Medicinal Plants Research*, 5(21), 5284–5290.
- Li, C., Yang, D., Zhao, Y., Qiu, Y., Cao, X., Yu, Y., Guo, H., Gu, X., and Yin, X. (2015). Inhibitory effects of isorhamnetin on the invasion of human breast carcinoma cells by downregulating the expression and activity of matrix metalloproteinase-2/9. *Nutrition and Cancer*, 67(7), 1191–1200.
- Lim, W. M., and Kumar, S. (2024). Guidelines for interpreting the results of bibliometric analysis: A sensemaking approach. *Global Business and Organizational Excellence*, 43(2), 17–26.
- Loo, Y. C., Hu, H.-C., Yu, S.-Y., Tsai, Y.-H., Korinek, M., Wu, Y.-C., Chang, F.-R., and Chen, Y.-J. (2023). Development on potential skin anti-aging agents of *Cosmos caudatus* Kunth via inhibition of collagenase, MMP-1 and MMP-3 activities. *Phytomedicine*, 110, 154643.
- Lou, J., Duan, H., Qin, Q., Teng, Z., Gan, F., Zhou, X., and Zhou, X. (2023). Advances in oral drug delivery systems: Challenges and opportunities. *Pharmaceutics*, 15(2), 484.
- Maennling, A. E., Tur, M. K., Niebert, M., Klockenbring, T., Zeppernick, F., Gattenlöhner, S., Meinhold-Heerlein, I., and Hussain, A. F. (2019). Molecular targeting therapy against EGFR family in breast cancer: Progress and future potentials. *Cancers*, 11(12), 1826.
- Martino, E., D’Onofrio, N., Balestrieri, A., Colloca, A., Anastasio, C., Sardu, C., Marfella, R., Campanile, G., and Balestrieri, M. L. (2024). Dietary epigenetic modulators: Unravelling the still-controversial benefits of miRNAs in nutrition and disease. *Nutrients*, 16(1), 160.
- Mei, C., Zhang, X., Zhi, Y., Liang, Z., Xu, H., Liu, Z., Liu, Y., Lyu, Y., and Wang, H. (2024). Isorhamnetin regulates programmed death ligand-1 expression by suppressing the EGFR–STAT3 signaling pathway in canine mammary tumors. *International Journal of Molecular Sciences*, 25(1), 670.
- Muñoz-Leiva, F., Viedma-del-Jesús, M. I., Sánchez-Fernández, J., and López-Herrera, A. G. (2012). An application of co-word analysis and bibliometric maps for detecting the most highlighting themes in the consumer behaviour research from a longitudinal perspective. *Quality and Quantity*, 46(4), 1077–1095.
- Nedeljković, M., Tanić, N., Prvanović, M., Milovanović, Z., and Tanić, N. (2021). Friend or foe: ABCG2, ABCC1 and ABCB1 expression in triple-negative breast cancer. *Breast Cancer*, 28(3), 727–736.
- Nickel, J., Gohlke, B.-O., Erehman, J., Banerjee, P., Rong, W. W., Goede, A., Dunkel, M., and Preissner, R. (2014). SuperPred: Update on drug classification and target prediction. *Nucleic Acids Research*, 42(W1), W26–W31.
- Olowosoke, C. B., Eze, C. J., Munir, A., Dada, O. O., Omolabake, K. E., Oke, G. A., Mounadi, N., Chtita, S., and Ibisani, T. A. (2024). Integrative study of phytochemicals for anti-fibroid

- agent: A perspective on protein networks, molecular docking, ADMET, simulation, DFT and bioactivity. *Chemical Physics Impact*, 8, 100412.
- Pires, B. R. B., Mencialha, A. L., Ferreira, G. M., Souza, W. F. de, Morgado-Díaz, J. A., Maia, A. M., Corrêa, S., and Abdelhay, E. S. F. W. (2017). NF-kappaB is involved in the regulation of EMT genes in breast cancer cells. *PLoS ONE*, 12(1), e0169622.
- Rafi, M., Hayati, F., Umar, A. H., Septaningsih, D. A., and Rachmatiah, T. (2023). LC-HRMS-based metabolomics to evaluate the phytochemical profile and antioxidant capacity of *Cosmos caudatus* with different extraction methods and solvents. *Arabian Journal of Chemistry*, 16(9), 105065.
- Rahman, H. A., Sahib, N. G., Saari, N., Abas, F., Ismail, A., Mumtaz, M. W., and Hamid, A. A. (2017). Anti-obesity effect of ethanolic extract from *Cosmos caudatus* Kunth leaf in lean rats fed a high fat diet. *BMC Complementary and Alternative Medicine*, 17(1), 122.
- Ren, Y., Wu, H., Tan, M., Chen, J., Duan, Z., Zhu, B., Ruan, X., Yu, Q., Li, S., Liu, X., Liu, Y., and Si, Y. (2024). Acetylation of MOB1 mediates polyphyllin II-reduced lysosome biogenesis in breast cancer by promoting the cytoplasmic retention of the YAP/TFEB coactivator complex. *Phytomedicine*, 122, 155152.
- Ru, J., Li, P., Wang, J., Zhou, W., Li, B., Huang, C., Li, P., Guo, Z., Tao, W., Yang, Y., Xu, X., Li, Y., Wang, Y., and Yang, L. (2014). TCMSP: A database of systems pharmacology for drug discovery from herbal medicines. *Journal of Cheminformatics*, 6(1), 13.
- Sahidin, I., Nohong, N., Manggau, M. A., Arfan, A., Wahyuni, W., Meylani, I., Malaka, M. H., Rahmatika, N. S., Yodha, A. W. M., Masrika, N. U. E., Kamaluddin, A., Sundowo, A., Fajriah, S., Asasutjarit, R., Fristiohady, A., Maryanti, R., Rahayu, N. I., and Muktiarni, M. (2023). Phytochemical profile and biological activities of ethylacetate extract of peanut (*Arachis hypogaea* L.) stems: In-vitro and in-silico studies with bibliometric analysis. *Indonesian Journal of Science and Technology*, 8(2), 217–242.
- Sarmoko, S., Novitasari, D., Toriyama, M., Fareza, M. S., Choironi, N. A., Itoh, H., and Meiyanto, E. (2023). Different modes of mechanism of gamma-mangostin and alpha-mangostin to inhibit cell migration of triple-negative breast cancer cells concerning CXCR4 downregulation and ROS generation. *Iranian Journal of Pharmaceutical Research*, 22(1), e138856.
- Seyedreihani, S. F., Tan, T.-C., Alkarkhi, A. F. M., and Easa, A. M. (2017). Total phenolic content and antioxidant activity of ulam raja (*Cosmos caudatus*) and quantification of its selected marker compounds: Effect of extraction. *International Journal of Food Properties*, 20(2), 260–270.
- Shannon, P., Markiel, A., Ozier, O., Baliga, N. S., Wang, J. T., Ramage, D., Amin, N., Schwikowski, B., and Ideker, T. (2003). Cytoscape: A software environment for integrated models of biomolecular interaction networks. *Genome Research*, 13(11), 2498–2504.
- Sharifuldin, M. M. A., Ismail, Z., Aisha, A. F. A., Seow, E. K., and Beh, H. K. (2016). Quantification of rutin, quercitrin and quercetin in *Cosmos caudatus* Kunth by reverse phase high performance liquid chromatography. *Quality Assurance and Safety of Crops and Foods*, 8(4), 617–622.

- Sherman, B. T., Hao, M., Qiu, J., Jiao, X., Baseler, M. W., Lane, H. C., Imamichi, T., and Chang, W. (2022). DAVID: A web server for functional enrichment analysis and functional annotation of gene lists (2021 update). *Nucleic Acids Research*, *50*(W1), W216–W221.
- Shirvanian, K., Vali, R., Farkhondeh, T., Abderam, A., Aschner, M., and Samarghandian, S. (2024). Genistein effects on various human disorders mediated via Nrf2 signaling. *Current Molecular Medicine*, *24*(1), 40–50.
- Shui, G., Leong, L. P., and Wong, S. P. (2005). Rapid screening and characterisation of antioxidants of *Cosmos caudatus* using liquid chromatography coupled with mass spectrometry. *Journal of Chromatography B*, *827*(1), 127–138.
- Solihah, P. A., Kaniawati, I., Samsudin, A., and Riandi, R. (2024). Prototype of greenhouse effect for improving problem-solving skills in science, technology, engineering, and mathematics (STEM)-education for sustainable development (ESD): Literature review, bibliometric, and experiment. *Indonesian Journal of Science and Technology*, *9*(1), 163–190.
- Sun, F., Liu, J., Xu, J., Tariq, A., Wu, Y., and Li, L. (2024). Molecular mechanism of Yi-Qi-Yang-Yin-Ye against obesity in rats using network pharmacology, molecular docking, and molecular dynamics simulations. *Arabian Journal of Chemistry*, *17*(1), 105390.
- Syahrani, R., Umar, A. H., Rahman, H. N., and Kusuma, W. A. (2023). Exploration of *Annona muricata* (Annonaceae) in the treatment of hyperlipidemia through network pharmacology and molecular docking. *Sains Malaysiana*, *52*(3), 899–939.
- Szklarczyk, D., Gable, A. L., Lyon, D., Junge, A., Wyder, S., Huerta-Cepas, J., Simonovic, M., Doncheva, N. T., Morris, J. H., Bork, P., Jensen, L. J., and Mering, C. von. (2019). STRING v11: Protein–protein association networks with increased coverage, supporting functional discovery in genome-wide experimental datasets. *Nucleic Acids Research*, *47*(D1), D607–D613.
- Tabti, K., Sbai, A., Maghat, H., Lakhliifi, T., and Bouachrine, M. (2024). Computational assessment of the reactivity and pharmaceutical potential of novel triazole derivatives: An approach combining DFT calculations, molecular dynamics simulations, and molecular docking. *Arabian Journal of Chemistry*, *17*(1), 105376.
- Tao, L., Zhou, Y., Luo, Y., Qiu, J., Xiao, Y., Zou, J., Zhang, Y., Liu, X., Yang, X., Gou, K., Xu, J., Guan, X., Cen, X., and Zhao, Y. (2024). Epigenetic regulation in cancer therapy: From mechanisms to clinical advances. *MedComm – Oncology*, *3*(1), e59.
- Tluli, O., Al-Maadhadi, M., Al-Khulaifi, A. A., Akomolafe, A. F., Al-Kuwari, S. Y., Al-Khayarin, R., Maccalli, C., and Pedersen, S. (2023). Exploring the role of microRNAs in glioma progression, prognosis, and therapeutic strategies. *Cancers*, *15*(17), 4213.
- Umar, A. H., Ratnadewi, D., Rafi, M., Sulistyaningsih, Y. C., Hamim, H., and Kusuma, W. A. (2023). Drug candidates and potential targets of *Curculigo* spp. Compounds for treating diabetes mellitus based on network pharmacology, molecular docking and molecular dynamics simulation. *Journal of Biomolecular Structure and Dynamics*, *41*(17), 8544–8560.

- Wang, P., Zhou, R., Zhou, R., Feng, S., Zhao, L., Li, W., Lin, J., Rajapakse, A., Lee, C.-H., Furnari, F. B., Burgess, A. W., Gunter, J. H., Liu, G., Ostrikov, K. (Ken), Richard, D. J., Simpson, F., Dai, X., and Thompson, E. W. (2024). Epidermal growth factor potentiates EGFR(Y992/1173)-mediated therapeutic response of triple negative breast cancer cells to cold atmospheric plasma-activated medium. *Redox Biology*, *69*, 102976.
- Wang, X., Chen, J., Tie, H., Tian, W., Zhao, Y., Qin, L., Guo, S., Li, Q., and Bao, C. (2023). Eriodictyol regulated ferroptosis, mitochondrial dysfunction, and cell viability via Nrf2/HO-1/NQO1 signaling pathway in ovarian cancer cells. *Journal of Biochemical and Molecular Toxicology*, *37*(7), e23368.
- Wellberg, E. A., Johnson, S., Finlay-Schultz, J., Lewis, A. S., Terrell, K. L., Sartorius, C. A., Abel, E. D., Muller, W. J., and Anderson, S. M. (2016). The glucose transporter GLUT1 is required for ErbB2-induced mammary tumorigenesis. *Breast Cancer Research*, *18*(1), 131.
- Widiyantoro, A., and Harlia, H. (2021). Antioxidant activity of leaves extract of kenikir (*Cosmos caudatus* Kunth) with various extraction methods. *Indonesian Journal of Pure and Applied Chemistry*, *3*(1), 9–20.
- Wu, Q., Kroon, P. A., Shao, H., Needs, P. W., and Yang, X. (2018). Differential effects of quercetin and two of its derivatives, isorhamnetin and isorhamnetin-3-glucuronide, in inhibiting the proliferation of human breast-cancer MCF-7 cells. *Journal of Agricultural and Food Chemistry*, *66*(27), 7181–7189.
- Xue, W., Yu, Y., Yao, Y., Zhou, L., Huang, Y., Wang, Y., Chen, Z., Wang, L., Li, X., Wang, X., Du, R., Shen, Y., and Xu, Q. (2024). Breast cancer cells have an increased ferroptosis risk induced by system xc⁻ blockade after deliberately downregulating CYTL1 to mediate malignancy. *Redox Biology*, *70*, 103034.
- Yan, S., Wang, Y., Chen, M., Li, G., and Fan, J. (2015). Deregulated SLC2A1 promotes tumor cell proliferation and metastasis in gastric cancer. *International Journal of Molecular Sciences*, *16*(7), 16144–16157.
- Yin Bok, C., Jun Low, E. K., Augundhooa, D., Ariffin, H., Bin Mok, Y., Qing Lim, K., Le Chew, S., Salvamani, S., Er Loh, K., Loke, C. F., Gunasekaran, B., and Tan, S.-A. (2023). Comprehensive review of *Cratogeomys* genus: Ethnomedical uses, phytochemistry, and pharmacological properties. *Pertanika Journal of Tropical Agricultural Science*, *46*(1), 213–241.
- Yusoff, N. A. H., Rukayadi, Y., Abas, F., Khatib, A., and Hassan, M. (2021). Antimicrobial stability of *Cosmos caudatus* extract at varies pH and temperature, and compounds identification for application as food sanitiser. *Food Research*, *5*(3), 83–91.
- Zheng, Z., Zeng, X., Zhu, Y., Leng, M., Zhang, Z., Wang, Q., Liu, X., Zeng, S., Xiao, Y., Hu, C., Pang, S., Wang, T., Xu, B., Peng, P., Li, F., and Tan, W. (2024). CircPPAP2B controls metastasis of clear cell renal cell carcinoma via HNRNPC-dependent alternative splicing and targeting the miR-182-5p/CYP1B1 axis. *Molecular Cancer*, *23*(1), 4.
- Zhu, X., Li, J., Ning, H., Yuan, Z., Zhong, Y., Wu, S., and Zeng, J.-Z. (2021). α -Mangostin induces apoptosis and inhibits metastasis of breast cancer cells via regulating RXR α -AKT signaling pathway. *Frontiers in Pharmacology*, *12*, 739658.